

CARBON AND CLAY NANOPARTICLES PROVOKE NUMEROUS  
RESPONSES IN *SALMONELLA ENTERICA* VAR.  
*TYPHIMURIUM* AND *ESCHERICHIA COLI*

THESIS

Presented to the Graduate Council  
of Texas State University-San Marcos  
in Partial Fulfillment  
of the Requirements

for the Degree

Master of SCIENCE

by

Alicia A. Taylor, B.S.

San Marcos, Texas  
December 2010

CARBON AND CLAY NANOPARTICLES PROVOKE NUMEROUS  
RESPONSES IN *SALMONELLA ENTERICA* VAR.  
*TYPHIMURIUM* AND *ESCHERICHIA COLI*

Committee Members Approved:

---

Robert McLean, Chair

---

Gary Beall

---

Nihal Dharmasiri

---

Yixin Zhang

Approved:

---

J. Michael Willoughby  
Dean of Graduate College

**COPYRIGHT**

by

Alicia A. Taylor

2010

## ACKNOWLEDGEMENTS

I would like to thank my advisor, Dr. Robert J. C. McLean for guidance as well as providing opportunities to excel both in my thesis work and as a teacher. I would like to express thanks to my committee members, Drs. Gary Beall, Nihal Dharmasiri, and Yixin Zhang. I would like to thank Dr. Beall for generously providing all nanoparticles for this study. I would like to acknowledge Dr. T. Wood (Texas A&M University), Dr. K. E. Sanderson (University of Calgary), and Dr. C.A. Nickerson (Arizona State University) for providing the strains used in this study. I would also like to generously thank Alissa Savage, Dr. J. Koke, and the Texas State Biology Imaging Lab, supported by NSF grants USE-9052039 and DBI-0821252, for help with acquiring the TEM images. Thanks to Jeff R. Troy and Dr. J. Veech for help with statistical analyses. Furthermore, I want to thank Dr. G. Aron for assisting with the fish cell cultures and the TCID<sub>50</sub> assay.

I would like to thank my lab mates, Mary Weber, Nihar Deb Adhikary, Tesfalem Zere, Weihua Chu, Amanda Duran, Chris Munoz, and Ashley Orr for their support. I would also like to show appreciation for the wonderful comments and ideas I received while attending conferences. Finally, I would like to thank my family and friends, especially my parents; without their support and encouragement none of my work would have been possible. In addition I want to thank my Thursday night Discussion group.

This work was supported by the ARP Grant and the Texas State University-San Marcos Biology Department.

This manuscript was submitted on September 10, 2010.

## TABLE OF CONTENTS

	<b>Page</b>
ACKNOWLEDGEMENTS .....	iv
LIST OF TABLES .....	vii
LIST OF FIGURES .....	viii
ABSTRACT .....	x
INTRODUCTION .....	1
<i>Research Objective</i> .....	1
<i>Nanoparticle Chemistry</i> .....	3
<i>Biological Effects and Uses of Nanoparticles</i> .....	6
<i>Ames Test</i> .....	9
<i>Oxidative Stress</i> .....	10
<i>Concluding Remarks</i> .....	12
MATERIALS AND METHODS .....	13
<i>Overall strategy</i> .....	13
<i>Strains and Culture Conditions</i> .....	13
<i>Ames Test</i> .....	14
<i>Toxicity Testing</i> .....	16
<i>Toxicity Test Conditions</i> .....	16
<i>Growth Curves</i> .....	17

<i>Transmission Electron Microscopy</i> .....	18
<i>Statistical Analysis</i> .....	19
RESULTS .....	20
<i>Ames Test</i> .....	20
<i>Toxicity Testing: LB Plates</i> .....	20
<i>Toxicity Testing: LB Broths</i> .....	21
<i>Transmission Electron Microscopy</i> .....	23
<i>Growth Curves</i> .....	24
DISCUSSION .....	26
<i>Ames Test</i> .....	26
<i>Toxicity Testing: LB Plates</i> .....	27
<i>Toxicity Testing: LB Broths</i> .....	27
<i>Growth Curves</i> .....	30
<i>Conclusions</i> .....	30
<i>Closing Remarks</i> .....	31
LITERATURE CITED .....	59

## LIST OF TABLES

<b>Table</b>	<b>Page</b>
1. Organisms used as inoculum species .....	35
2. Davis minimal media recipe .....	35
3. LB broth toxicity test requirements for tests, controls, and blanks .....	36
4. Concentrations of nanoparticles used in the LB broth toxicity tests .....	36

## LIST OF FIGURES

Figure	Page
1. Carbon nanotube structure .....	33
2. Montmorillonite clay structure .....	34
3. Transmission electron microscope image of halloysite nanotubes.....	34
4. LB toxicity tests under light conditions .....	36
5. Ames test <i>Salmonella typhimurium</i> TA102.....	37
6. Ames test <i>S. typhimurium</i> TA1537.....	37
7. Ames test <i>S. typhimurium</i> TA1538.....	38
8. LB toxicity test (plate) <i>S. typhimurium</i> TA102 .....	38
9. LB toxicity test (plate) <i>S. typhimurium</i> TA1537 .....	39
10. LB toxicity test (plate) <i>S. typhimurium</i> TA1538 .....	39
11. LB toxicity test (broth) <i>Escherichia coli</i> BW25113 .....	40
12. LB toxicity test (broth) <i>E. coli</i> BW25113 <i>oxyR</i> .....	41
13. LB toxicity test (broth) <i>E. coli oxyR/pCA24N</i> .....	42
14. LB toxicity test (broth) <i>E. coli oxyR/pCA24N-oxyR</i> .....	43
15. LB toxicity test (broth) <i>E. coli</i> MG1655.....	44
16. LB toxicity test (broth) <i>E. coli</i> ZK1000.....	45
17. LB toxicity test (broth) <i>S. typhimurium</i> TA102.....	46
18. LB toxicity test (broth) <i>S. typhimurium</i> TA1537.....	47
19. LB toxicity test (broth) <i>S. typhimurium</i> TA1538.....	48

20. LB toxicity test (broth) <i>S. typhimurium</i> LT-2.....	49
21. LB toxicity test (broth) <i>S. typhimurium</i> SGSC 1336 <i>oxyR</i> .....	50
22. LB toxicity test (broth) <i>S. typhimurium</i> SGSC 2618 <i>rpoS</i> .....	51
23. Transmission electron images of the Cloisite®, HNT, and MWCNTs with and without <i>Salmonella typhimurium</i> LT-2.....	52
24. <i>E. coli</i> BW25113 (wt) growth curve.....	53
25. <i>E. coli</i> BW25113 <i>oxyR</i> growth curve .....	53
26. <i>E. coli oxyR/pCA24N</i> growth curve .....	54
27. <i>E. coli oxyR/pCA24N-oxyR</i> growth curve .....	54
28. <i>E. coli</i> MG1655 growth curve .....	55
29. <i>E. coli</i> ZK1000 growth curve.....	55
30. <i>S. typhimurium</i> TA102 growth curve.....	56
31. <i>S. typhimurium</i> TA1537 growth curve.....	56
32. <i>S. typhimurium</i> TA1538 growth curve structure.....	57
33. <i>S. typhimurium</i> LT-2 growth curve.....	57
34. <i>S. typhimurium</i> SGSC 1336 <i>oxyR</i> growth curve.....	58
35. <i>S. typhimurium</i> SGSC 2618 <i>rpoS</i> growth curve .....	58

## ABSTRACT

CARBON AND CLAY NANOPARTICLES PROVOKE NUMEROUS  
RESPONSES IN *SALMONELLA ENTERICA* VAR.  
*TYPHIMURIUM* AND *ESCHERICHIA COLI*

by

Alicia A. Taylor, B.S.

Texas State University-San Marcos

December 2010

SUPERVISING PROFESSOR: ROBERT J. C. MCLEAN

Nanoparticles are classified by having at least one dimension of the particle measuring less than 100 nm. Due to their large surface area to volume ratio, nanoparticles may have unusual and unique properties not attributed to larger particles, and are often be more reactive. Nanoparticles have become widely used in many products in the past twenty years, including cosmetics, paints, clothing, electronics, and medical equipment. Because nanoparticles are becoming increasingly common and widespread, it is crucial to recognize not only how these particles can impact human health and the environment, but it is fundamental to understand how nanoparticles affect organisms on a smaller scale, such as bacteria. The studies described here focused on multiple *Escherichia coli* and *Salmonella enterica* var. *typhimurium* strains. Using the Ames test, increasing concentrations of three nanoparticles were examined to detect a mutagenicity effect. Multi-walled carbon nanotubes, halloysite nanotubes, and Cloisite® Na<sup>+</sup> nanoparticles were tested and it was found that the nanoparticles did not have a true mutagenic effect, although all three nanoparticles exhibited potential for weak toxicity effects. Further toxicity tests were conducted under light, dark, aerobic, and anaerobic conditions,

demonstrating that the nanoparticles resulted in levels of toxicity that varied according to strain. Some nanoparticles appeared to possibly elicit oxidative stress in *S. typhimurium*, as evidenced by decreased survival of *S. typhimurium* SGSC 1336 *oxyR*- when treated with the multi-walled carbon nanotube ( $P < 0.001$ ). This study concludes that nanoparticles may not have a general toxic effect across all bacterial species; rather species-specific responses are demonstrated.

## INTRODUCTION

### *Research Objective*

A nanoparticle (NP) is classified as having at least one dimension 100 nm in size or less (41). Because of their size, nanoparticles have a high surface area to volume ratio, which gives the particles unique and unusual properties, often making them more reactive (21, 41). Nanotechnology has become a hot topic in research and it is expected by 2015, nanotechnology will be a one trillion dollar industry. Nanoparticles are presently being used in electronics and other technological tools, as well as commercially available cosmetics, paint products, fillers, opacifiers, catalysts, semiconductors, sporting goods equipment, tires, stain resistant clothing, and as diagnostics and imaging tools (6, 35, 41). Importantly, nanoparticles can be further modified by adding side chains or other components that can affect the size, shape, surface chemistry, surface area, charge, hydrophobicity, and purity of the particle (45).

Some research has been conducted on nanoparticles and environmental and health concerns (6, 14). One environmental concern is the trophic transfer of nanoparticles in the food web (18). Because the potential toxicity is not known, as well as the possible synergistic effects with other already present compounds, nanoparticles may be inducing mutations in organismal DNA, ranging from bacteria to humans (44, 5). This research is relevant to medical studies because nanoparticles may be unsafely interacting with other compounds, or may have a negative effect solely on their own. This could be important for cancer related fields (21). There have been thousands of studies over the past decades

on other pollutants in the environment and the undesirable effects they cause on organisms as well as people. Nanoparticles may or may not have a synergistic effect with these already transpiring compounds. However, due to limited research, it is not certain if nanoparticles are able to enter the food web and transfer between trophic levels (27).

Nanoparticles occur naturally in the environment, however industrially made nanoparticles have only been around a short time. There is little research on the potentially adverse effects of these particles (37). As these nanoparticles penetrate our watersheds, they will come into contact with other pollutants, such as endocrine disruptors, organic wastes, and over abundant nutrients such as potassium and sodium. Nanoparticles do have the ability to cause harm to multiple organisms and ecological systems (5, 8, 10, 11, 12, 13, 14, 16, 21, 26, 28, 30, 41, 43, 48); and currently new research is investigating the budding concerns.

Some preliminary Ames assays have been performed with metal nanoparticles (FePt and metallic oxides), but these studies showed limited mutagenicity of the metals (32, 49). As nanotechnology becomes more prevalent, it is important to develop a complete understanding of the potential issues associated with nanoparticles, such as toxicity and mutagenicity as well as possible concerns involving nanoparticles in watersheds and food chains. Using the Ames test and other supplemental toxicity testing, this study aims to investigate three nanoparticles: multi-walled carbon nanotubes (MWCNT), halloysite nanotubes (HNT), and Cloisite® Na<sup>+</sup> nanoparticles (Cloisite®), and their effects on multiple strains of bacteria.

### *Nanoparticle Chemistry*

Carbon nanotubes are categorized either as single-walled carbon nanotubes (SWCNT) or as multi-walled carbon nanotubes (MWCNT). The MWCNTs consist of multiple rolled layers of graphene with the interlayer distance close to the distance between graphene layers in graphite, approximately 3.4 Å (Figure 1). MWCNTs were tested to have a tensile strength of 63 gigapascals, which is the second highest tensile strength of any material yet measured (60). Carbon nanotubes are some of the strongest and stiffest materials available for product development, making it an ideal material for many manufactured goods. Carbon nanotubes are in the fullerene structural family (includes Buckminsterfullerenes) and their name is derived from their size, the diameter being 1/50,000<sup>th</sup> of the width of a human hair and as of 2010, the length reaching up to 18 cm in length (58). Nanotubes have been constructed with length-to-diameter ratio of up to 132,000,000:1 (58).

This particular nanoparticle is very popular in numerous areas of research, ranging from electronics, polymer fibers created by electrospinning, electrochemical durability testing, uses as electrodes and for biosensing, optics, materials science, thermal conductors, nanoelectrode arrays for ultrasensitive DNA detection, and for efficient molecular delivery into mammalian cells using carbon nanotube spearing (39). Specifically, the multi-walled carbon nanotubes used in this study (NanoLab, Inc., Catalog number IG-25g) were produced via the chemical vapor deposition (CVD) method and the estimated purity of the product is >85 Wt%. The known impurities include iron and ceramic oxides (39). The diameter has a range of 10-30 nm and the

length spans from 5-20  $\mu\text{m}$  nominal. Some of its physical properties include water insolubility and it has an unknown melting point (4).

The second nanoparticle used in this study is montmorillonite clay (Figure 2). The smectite clay family which includes montmorillonite is classified as a 2:1 phyllosilicate clay, and has a unit crystal lattice formed by one alumina octahedral sheet sandwiched between two silica tetrahedral sheets. The interlayer between units contains positive cations and water molecules. Due to this crystalline arrangement, smectites are able to expand and contract the interlayer while maintaining a two dimensional crystallographic integrity. The clays are characterized by octahedral and/or tetrahedral substitution and high ion exchange capacities (33). Chemically, montmorillonite is hydrated sodium calcium aluminum magnesium silicate hydroxide  $(\text{Na}, \text{Ca})_{0.3}(\text{Al}, \text{Mg})_2\text{Si}_4\text{O}_{10}(\text{OH})_2 \cdot n\text{H}_2\text{O}$  (3). However, other cations can be substituted; the exact ratios are dependent on the source of the clay (3).

Montmorillonite clays have a high cation exchange capacity on their surface (17) as well as an ability to swell in aqueous environments. These attributes make these clays ideal as absorbents. Montmorillonite clays are known for its absorbent qualities and can be used as soil additives for water retention in drought prone areas as well as an additive in cosmetics (9, 33). The surface chemistry of montmorillonite clays can be altered by exchanging the predominant interlaminar cations with materials that are positively charged (such as sodium) (17). The further addition of organic cations in excess of the exchange capacity of the clay results in an organoclay with a positive instead of negative surface charge (17).

The Cloisite® Na<sup>+</sup> nanoparticle, manufactured by Southern Clay Products, Inc., is a natural montmorillonite and is specifically used for reinforcement and modification of physical properties in plastics, such as heat deflection temperature (HDT) and coefficient of linear thermal expansion (CLTE) (51). At ambient temperatures, this clay product is 4-9 w/w% moisture. Typical dry particle sizes are 90% (by volume) with a size <13µm, while 50% are below 6µm, and 10% are 2µm or smaller. The density of this product is 2.86 g/cc (51). This product has been shown to improve the properties of injection molded pieces for the automotive industry, of flexible and rigid packaging such as films, bottles, trays, and blister packs, and also of electronics plastics such as wire and cable coatings (51).

The final nanoparticle used for this study, a halloysite nanotube, is also a natural clay aluminosilicate mineral (Figure 3). It is made from aluminum, silicon, hydrogen, and oxygen; its formula is Al<sub>2</sub>Si<sub>2</sub>O<sub>5</sub>(OH)<sub>4</sub> (2). Halloysite typically forms by hydrothermal alteration of alumino-silicate minerals (23). Halloysite is a two-layered clay, consisting of one alumina octahedron sheet and one silica tetrahedron sheet in 1:1 stoichiometric ratio. It is chemically similar to kaolin, differing mainly in the morphology of crystals (22). Halloysite clays can occur intermixed with other clays, particularly montmorillonites (23). The versatile and natural halloysite nanotubes are made from millions of years of surface weathering of these clay minerals (40). Halloysite nanotubes are minuscule hollow tubes with diameters in general smaller than 100 nm, with lengths ranging from about 500 nm to over 1.2 µm (40).

Like montmorillonite, halloysite is considered a low cost absorbent clay (31) Halloysite nanotubes (HNTs) possess hollow nanotubular structure in the submicrometer

range and large specific surface area. Their novel physical and chemical properties derived from the structural versatility provide opportunities for advanced applications in fields such as electronics, catalysis, biological systems, and functional materials (22). In contrast with other nano-sized materials, naturally occurring HNTs are readily obtainable and much cheaper than other nanoparticles such as carbon nanotubes (CNTs). More importantly, the unique tubular structure of HNTs resembles that of CNTs. Therefore, HNTs may have the potential to provide cheap alternatives to the expensive CNTs for dye removal (46). One study conducted by Luo et al. (2010) concluded that HNTs could be used as a low-cost and relatively effective adsorbent for the removal of Neutral Red dye from wastewater (31).

#### *Biological Effects and Uses of Nanoparticles*

The toxicological and ecological effects of the multi-walled carbon nanotubes have not been thoroughly researched. However, the toxicity of pristine and oxidized multi-walled carbon nanotubes on human T cells was studied and it was found that oxidized MWCNTs are more toxic and can induce massive loss of cell viability through programmed cell death at doses of 400  $\mu\text{g/mL}$ ; this corresponds to approximately 10 million carbon nanotubes per cell. These results suggest that MWCNTs can be very toxic at sufficiently high concentrations and that careful toxicity studies need to be undertaken particularly in conjunction with nanomedical applications of carbon nanotubes (8). Other studies have shown that fullerene nanomaterials induce oxidative stress in the brain of juvenile Largemouth Bass (43) and can inhibit the allergic response in the immune system (48). Epidemiological studies have shown that ultra-fine particles are considered to play a role in mediating the adverse effects in patients with cardiovascular and

respiratory diseases (11); it is of increasing concern that human exposure to some types of engineered nanoparticles may lead to significant adverse health effects.

Montmorillonite clays suspended in aqueous solution at physiological pHs are negatively charged (42). Most bacterial cells under physiological conditions also have negatively charged surfaces (53). Therefore, bacteria and clays in suspension should mutually repel each other. Exchanging montmorillonites with cationic surfactants produces materials that are more hydrophobic (42). Hydrophobic and electrostatic interactions, van der Waals forces, and cation bridging have been implicated as the major forces associated with the attachment of bacteria to clay and soil particles (56). Bacteria have strain-specific differences in surface hydrophobicity and electrostatic charge and thus vary in the surfaces to which they are attracted (17).

The effects of montmorillonite clays on bacteria have been carefully studied. Khanna and Stotzky showed that the charges associated with the montmorillonite clays assist cryptic genes to persist in the environment when bound on particulates, such as montmorillonite clay, thereby facilitating efficient transformation (25). DNA can be adsorbed and bound on montmorillonite; the bound DNA retains the capability of transforming competent cells, and also the bound DNA is more resistant to degradation. These results support the concept of the occurrence of cryptic genes bound on particulates in the environment. Cryptic genes may persist undetected in soils but be subsequently expressed when a susceptible host comes into contact with the clay-DNA complexes and transformation occurs (25).

Furthermore, antibacterial compounds, such as silver ions, have been immobilized on montmorillonite clays and then released through ion exchanges with sodium; this

demonstrates the clay's ability to be used as a carrier for antibacterials as well as its possible storage mechanism of compounds due to intercalation (34). Clay minerals have shown little to no effect on bacteria, but can absorb and kill bacteria when antibacterial compounds are intercalated (38). Early studies on copper montmorillonite clay have shown to have antibacterial effects on *Escherichia coli* K88 (19). It has been shown that metallic ion-exchanged montmorillonite dispersed in water attracts and adsorbs negatively charged bacteria, improving the antibacterial properties of the material (20).

Finally, NaturalNano is currently developing techniques to separate halloysite nanotubes by size; this feature will make the nanotubes available for numerous commercial applications, such as additives in polymers and plastics, cosmetics, electronic components, and home and personal care products (40). The functional qualities desired for such commercial applications are controlled through selection of the tube diameter and length. Furthermore, halloysite nanotubes can be coated with metals and other substances to make the tubes more applicable for electrical and chemical uses. The nanotubes can also be saturated with active ingredients that can be pertinent for uses like cosmetics, pesticides, pharmaceuticals, and other extended release compounds (40). Currently, NaturalNano has begun research with Biophan Technologies, Inc. to use halloysite nanotubes as a vehicle for drug delivery technologies (40). Biophan also uses the nanotubes for a range of other products, such as bandages and wound healing applications and in controlled release technology for a range of active agents (40). NaturalNano also has prototypes for various products that incorporate the halloysite nanotube, such as a nanotube enriched paint that can block radio frequency signals (40).

### *Ames Test*

The Ames test was developed by Bruce Ames of The University of California-Berkeley in 1973 (1). This assay detects for potential mutagenic compounds by engineering *Salmonella typhimurium* to have a more permeable cell membrane, a defective DNA repair system and mutated histidine genes (37, 1, 36). The Ames strains were initially derived from a parent strain called *S. typhimurium* strain LT-2. There are multiple Ames strains; each strain has a different mutation in one of the eight histidine genes and can detect for different types of mutations as well as mutagenic conditions, such as oxidative stress. Because each of the strains has a mutated histidine gene, the strains are no longer capable of producing their own histidine. The Ames test is performed on a minimal media that lacks histidine; therefore the strains do not grow unless the mutagenic compound causes the histidine genes to spontaneously revert (1). The revertant colonies are then counted and the mutagen may be identified as a mutagenic or carcinogenic compound.

*Salmonella typhimurium* TA1537 has an insertion frameshift mutation in the histidine C gene (codes for histidinol phosphate aminotransferase). The mutated gene is called hisC3076. The wildtype gene at base pair 3076 reads 'ccc' while the mutation reads 'cccc' (1). *Salmonella typhimurium* TA1538 has a deletion frameshift mutation in histidine D gene (codes for histidinol dehydrogenase). The mutated gene is called hisD3052 and contains a 'cc' while the wildtype contains 'ccc' (1). *Salmonella typhimurium* TA102 has a nonsense mutated histidine G gene called hisG8476. HisG codes for ATP phosphoribosyl transferase and at base 1522 the mutated strain contains a 't' instead of a 'c' (27).

### *Oxidative Stress*

Bacteria, like other living organisms, have developed defense systems against oxidative stress. In *Escherichia coli* and related bacteria, *OxyRS* and *SoxRS* are the key regulators of the transcriptional oxidative stress response to (hydrogen) peroxide and superoxide, respectively (52). *Salmonella* is a gram negative, facultative intracellular pathogen that is associated with gastroenteritis, septicemia, and typhoid fever (15). The survival ability of *Salmonella* strains after exposure to oxidative stress demonstrates that proteins perform a pivotal function in the survival of stationary-phase *S. typhimurium* against oxidative stress (59). The Dps protein plays a critical role in protecting DNA from oxidative stresses in stationary phase. Also, *Salmonella* is able to augment its resistance to phagocyte-derived reactive oxygen species (ROS) via the induction of several pathways that are controlled by a number of regulatory systems, including *OxyRS*, *SoxRS*, and *RpoS* (59).

Oxidative cell damage will occur, for example, when hydrogen peroxide ( $\text{H}_2\text{O}_2$ ) accumulates in the cell. Because of aerobic respiration, oxidants such as  $\text{H}_2\text{O}_2$  are generated in living organisms by normal cellular metabolism.  $\text{H}_2\text{O}_2$  is normally disposed of by specialized enzymes, such as catalases and peroxidases, so that its concentration remains at a level beneficial to the cell. Indeed, in small concentrations ( $10^{-6}$  M),  $\text{H}_2\text{O}_2$  is a signaling molecule capable of inducing chemotactic activity, stimulating the synthesis of cytoskeleton elements, and causing changes in cytosolic calcium concentrations. However, physiological perturbations of cellular homeostasis may lead to a dramatic increase in the amount of  $\text{H}_2\text{O}_2$  within a cell. In the presence of transition metals,  $\text{H}_2\text{O}_2$  is rapidly converted to the highly reactive and highly toxic hydroxyl radical ( $\text{OH} \cdot$ ). The

latter is responsible for lipid peroxidation, oxidative damage to proteins, and breakage of DNA strands (24) During the reduction of oxygen to water in aerobic life, superoxide radicals ( $O_2 \cdot^-$ ),  $H_2O_2$ , and  $OH \cdot$ , all known as reactive oxygen species (ROS), can be formed.  $O_2 \cdot^-$  is a moderately reactive ROS that is readily dismutated to  $H_2O_2$ . It is also able to reduce metal ions that are mainly present in the cell in the oxidized form (24). Superoxide dismutases, located in the bacterial periplasm and in the cytoplasm, dismutate superoxide  $O_2$  to hydrogen peroxide,  $H_2O_2$ , and molecular oxygen (29). The *KatE* and *KatG* catalases are involved in  $H_2O_2$  degradation, with *katE* being described as a member of the *RpoS* regulon and *katG* being *OxyR* (29). Both enzymes share the ability to reduce hydrogen peroxide to water and molecular oxygen, and their role was shown to be predominant at millimolar concentrations of  $H_2O_2$  since they do not require any reductant (50).

$TiO_2$  nanoparticle (NP) toxicity has been studied with respect to reactive oxygen species (ROS) production and oxidative stress in mammalian studies.  $TiO_2$  NPs induced oxidative damage to human bronchial epithelial cells (13) and to brain microglia (30). Some ecological studies showed that  $TiO_2$ NP exposure in aquatic species caused oxidative damage-mediated effects (12). The exposure of rainbow trout (*Oncorhynchus mykiss*) to  $TiO_2$  NPs caused lipid peroxidation, one of the consequences of oxidative stress, in the gill, intestine and brain (12) and changes in antioxidant enzyme activities were observed in terrestrial isopods (*Porcellio scaber*) and freshwater cladoceran (*Daphnia pulex*) (26). To date, several studies have investigated the toxic effects of silica nanoparticles in vitro and in vivo. These reports demonstrated that silica nanoparticles were capable of producing reactive oxygen species (ROS), leading to cytokine release

and apoptosis in macrophage cell (16). Moreover, it was reported that ROS-mediated oxidative stress played an important role in toxicity of nanoparticles (10, 28, 41).

Nanoparticles may cause toxicity to bacteria through reactive oxygen species (ROS) that are created in the presence of light. Nakagawa (1997) showed that TiO<sub>2</sub> particles showed no toxicity in a chromosomal aberration assay, but with UV and visible light TiO<sub>2</sub> particles demonstrated significant photogenotoxicity (61). Nanoparticles may have the potential to be photogenotoxic.

#### *Concluding Remarks*

Nanoparticles are believed to create reactive oxygen species (ROS) in the presence of light and under light conditions stronger toxicity trends may be present. This study will examine reactive oxygen species and oxidative stress responses of several strains of *S. typhimurium* and *E. coli* to the nanoparticles and will include both aerobic and anaerobic tests with and without light. This will investigate if ROS are responsible for the toxic effect on the bacteria. Ames Tests, LB toxicity tests (with both plated and liquid broth), and growth curves will be conducted under numerous conditions (aerobic/anaerobic and light/dark). Because *S. typhimurium* and *E. coli* are facultative anaerobes, all strains will be examined under anaerobic conditions because of their distinctive metabolic abilities.

## MATERIALS AND METHODS

### *Overall Strategy*

This research described toxicity effects of the three nanoparticles on numerous strains of bacteria (Table 1). The Ames test was used to assess mutagenicity effects of the nanoparticles. LB toxicity tests (both with plated and liquid mediums) were run to determine bacterial cell death at varying concentrations of nanoparticles. Transmission electron microscopy imaging was utilized to observe bacteria in the presence of the nanoparticles. Toxicity testing was further performed to assess any harmful effects associated with the three nanoparticles. Toxicity tests were performed with LB (Luria-Bertani) plates and with LB broths. Strains underwent four treatments during the LB broth testing: aerobic, anaerobic, light, and dark. The bacterial strains applied to this study were both *Escherichia coli* and *Salmonella enterica var. typhimurium*.

### *Strains and Culture Conditions*

All strains used in this study were grown at 37 °C. For preparing Ames strains, samples were streaked onto Nutrient Agar (NA) plates and incubated for 24 hrs in a 37°C incubator. All other strains required an LB medium for growth. The plates were then transferred to the refrigerator for further storage. Glycerol stocks were made of each strain and stored at -80 °C. New stock plates were made once a week. Some strains had specific antibiotic requirements (Table 1). Antibiotics were made according to strain requirements and filter sterilized before use. For more detailed information on strains and their requirements, see table 1.

### *Ames Test*

A stock solution of nanoparticles (NP) was made the following way: 0.1 g of the nanoparticle was weighed and added to 10 mL of deionized water. The suspension was sonicated for two minutes at an output of 2 with a constant rate until thoroughly mixed with a probe sonicator (Branson, sonifier model 250). The solution was then autoclaved for 15 minutes at 15 psi at 121 °C. Serial dilutions were then made. Sterile test tubes were filled with 9 mL of sterile Millipore water. 1 mL of the NP stock solution was aseptically transferred to tube 1. A new pipette tip was used to gently mix the solution and 1 mL was transferred to tube 2. Further dilutions were made accordingly. This procedure was used for all serial dilutions of the nanoparticles unless otherwise mentioned.

To prepare MWCNTs suspensions, Polyvinylpyrrolidone (PVP) was added to the 0.1g of MWCNTs before addition to the 10 mL of Millipore water. This was done to reduce the hydrophobicity of the MWCNT and created easier dispersion of the MWCNTs in the Millipore water. A 10% Polyvinylpyrrolidone (g/v) was prepared using water and vortexed thoroughly. This solution was sprayed into 0.1g of the MWCNTs 10 times (roughly 1 mL). After addition of the PVP spray, the sample was sonicated and autoclaved.

The Davis Minimal Agar (DMA) used for the Ames test was made according to Table 2. Sterile Petri plates were labeled with appropriate NP dilution numbers. Plates labeled with  $10^{-1}$  dilution factor had 1 mL of the solution from test tube 1. The solution was aseptically transferred to the bottom of the Petri plate. The DMA was poured over the nanoparticle solution and the Petri plate was gently mixed in a clockwise motion three times and then in a counterclockwise motion three times. The other dilution Petri plates

were arranged in the same manner. Plates were allowed to solidify and were monitored for contamination for 24 hrs after pouring. The above steps were performed for each nanoparticle.

Negative controls were made by pouring Davis Minimal Agar into Petri plates without adding the nanoparticle solution. Two positive controls were made: dimethyl sulfoxide (DMSO) and sodium azide controls. DMSO was poured into a screw cap bottle and autoclaved, the DMSO was not diluted. The sodium azide was carefully measured with a weigh boat using the Mettler Toledo PB602 Digital Scale. 0.1 g of sodium azide was placed into 100 mL of Phosphate Buffered Saline (PBS) and then the solution was autoclaved. To make the control plates, 1 mL of the individual solutions were transferred to separate Petri plates and the DMA was poured over. Again, the plate was rotated clockwise and counterclockwise to properly mix the solution into the media.

When plating Ames strains, the strains were grown overnight in 5 mL of Nutrient Broth. Side arm flasks were sterilized and 50 mL of nutrient broth was aseptically transferred to each flask. 50  $\mu$ L of the overnight Ames broths were transferred to the side arm flasks. The flasks were placed in the 37 °C incubator and shaken at 100 rpm. Strains reached an optical density ( $OD^{600}$ ) of 0.3 and the OD was verified with a spectrophotometer (Spectronic 20D+, Thermo Scientific). Using growth curves, the time taken each strain to reach  $OD^{600} = 0.3$  was determined. Strains were utilized in experiments with an optical density of 0.3.

100  $\mu$ L of a bacterial strain was plated onto the Ames tests and control plates to assess the mutagenic potential of the chemical compounds. Plates were kept upright for five minutes after plating and were then transferred into a 37 °C incubator and placed

upside down for 48 hrs. Colonies were counted on each plate using a Colony Counter (Darkfield Quebec). Colony forming units (CFU) were then established.

### *Toxicity Testing*

Toxicity tests were set up as following (Table 3): 4.5 mL of LB broth was added to a sterile test tube. The tenfold nanoparticle serial dilutions previously made were also used for this experiment. From the premade dilutions, 0.5 mL was removed and aseptically added to the test tube. Test tubes were not used for 24 hours to monitor for contamination. Bacterial strains were grown overnight and then 50  $\mu$ L was added to 50 mL of LB broth in a side arm flask. Bacteria were allowed to grow to 0.3 OD<sup>600</sup>. To inoculate the toxicity tests, 25  $\mu$ L of the strain was added to each test tube. Tests were run in 37 °C conditions for 24 hours. To record data, 1.0 mL of each toxicity test was aliquoted into a cuvette and absorbance at OD<sup>600</sup> was measured using a spectrophotometer (SmartSpec<sup>TM</sup> Plus, Bio-Rad). Blanks were used for each defined nanoparticle concentration. Each of the three nanoparticles was tested for toxicity on all strains of bacteria (Table 1).

To verify results seen with toxicity tests under LB broth conditions, toxicity tests were also performed with LB agar plates. To prepare, this toxicity test was assembled in an identical manner to the Ames test, the only difference being that LB agar was used instead of Davis Minimal agar. Nanoparticle serial dilutions were identical to the Ames test as well as the addition of nanoparticle solutions to the Petri dishes.

### *Toxicity Test Conditions*

Broth toxicity tests were run under four conditions: aerobic, anaerobic, light, and dark. To simulate anaerobic conditions, after inoculating toxicity tests, 1.0 mL of sterile

mineral oil was added aseptically to the test tube. The control used for this set of anaerobic tests included 5 mL of LB broth inoculated with 25  $\mu$ L of the strain grown overnight and 1 mL of mineral oil added as a layer over the LB broth. Each toxicity test consisted of four different concentrations of nanoparticles with three replicates as well as three aerobic and three anaerobic controls for each test (Table 4). Aerobic tests were performed without the use of mineral oil and appropriate controls were made.

Light tests were set up using four 60 watt light bulbs arranged in four points around the toxicity test tube racks in a 37 °C incubator. Light bulbs were roughly 5 inches away from the tests (Figure 4). Both aerobic and anaerobic tests were performed under light conditions. To prepare dark tests, toxicity test tube racks, both aerobic and anaerobic tests, were placed in a large styrofoam ice chest and placed in the 37 °C incubator. The ice chest lid was placed securely on top to reduce all light inside the ice chest. To confirm proper temperature conditions, thermometers were placed with the light and dark tests.

### *Growth Curves*

50 mL of LB broth was transferred to 12 side arm flasks. Treatments were prepared accordingly: the control contained 50 mL LB broth plus an additional 2 mL of LB, treatment 1 contained 50 mL LB broth and 2 mL of the  $10^{-1}$  g Cloisite® solution, treatment 2 contained 50 mL LB broth and 2 mL of the  $10^{-1}$  g HNT solution, and treatment 3 contained 50 mL LB broth and 2 mL of the  $10^{-1}$  g MWCNT solution. After adding bacteria and nanoparticles, each flask contained a total of 52.25 mL. Two side arm flasks were made for each treatment as two replicates. Additionally, one control for each of the treatments was arranged identically. Bacteria was grown in 5 mL LB broth

overnight at 37 °C and then 250 µL was added to all treatments and replicates. All side arm flasks were placed in a 37 °C incubator at 100 rpm. Absorbance at 600 nm was read hourly for the first 12 hours and hours 24, 36, 48, 60 and 72 on using a spectrophotometer (Spectronic 20D+, Thermo Scientific). Before sampling, the spectrophotometer was blanked with the appropriate control. The LB flasks had a blank consisting of 500 µL of LB only, while each nanoparticle flask was blanked with 500 µL of the original suspension inside of the growth curve flask, before adding bacteria.

#### *Transmission Electron Microscopy*

Three samples of *S. typhimurium* LT-2 LB toxicity tests were prepared with nanoparticle concentrations of  $10^{-2}$  g. Samples were grown for 24 hrs. To prepare for imaging, 1-2 µL of each sample was removed and placed on the top of a formvar carbon film on 200 square mesh copper grids. The grid was then allowed to dry. To fix the sample, a small drop of 2% uranyl acetate was placed on parafilm inside a Petri plate. The grid was placed section side down on the drop of 2% uranyl acetate and left for three minutes. Next, the grid was flipped right side up and a small piece of filter paper was used to absorb excess uranyl acetate. The grid again was allowed to dry and was viewed using a JEOL transmission electron microscope (model JEM 1200 EX 2) with a Gatan digital camera. Three nanoparticle control samples were also viewed. To prepare, 0.5 mL of each nanoparticle was taken from the stock solution (0.1 g nanoparticle / 10 mL Millipore water) and placed in a test tube with 4.5 mL Millipore water. Control samples were prepared identical to the bacterial samples except controls were not exposed to uranyl acetate. All samples were imaged by Alissa Savage.

### *Statistical Analysis*

Statistical analyses were completed only for LB broth toxicity tests. Statistical analyses and graphs were completed using SigmaPlot 11.0 (55). Failure to obey assumptions of normality and homoscedasticity required the use of a Kruskal-Wallis test (non-parametric ANOVA). The Holm-Sidak *t*-test was used for multiple comparisons following the Kruskal-Wallis results. Each LB toxicity test was performed with two controls (aerobic and anaerobic); however, only the appropriate control was statistically analyzed (i.e., for aerobic tests, only the aerobic control was included in analyses and vice versa for anaerobic tests). Tests were considered significant if  $P < 0.05$ .

## RESULTS

### *Ames Test*

All Ames strains were exposed to  $10^{-2}$  g to  $10^{-13}$  g of all three nanoparticles and strains demonstrated different responses when in the presence of the each nanoparticle.

*Salmonella typhimurium* TA102 exhibited less growth in the presence of the nanoparticles and showed possible mutagenic capabilities. TA102 exhibited less growth with nanoparticle treatments of HNT when compared to the negative control; this showed that there may be potential for toxicity effects (Figure 5). *Salmonella typhimurium* TA1537 also showed no significant correlation between mutagenic or toxic effects of the nanoparticles when the treatments were compared to the negative control (Figure 6). *Salmonella typhimurium* TA1538 showed slightly higher CFUs for the Cloisite® when compared to the control, but CFUs were not high enough to show significance for mutagenicity. When exposed to HNT and MWCNTs, TA1538 demonstrated less growth compared to the control, suggesting that these two NPs may be potentially toxic to TA1538 (Figure 7).

### *Toxicity Testing: LB Plates*

The LB toxicity tests (plates) demonstrated that the nanoparticles may have some potential for a toxicity effect. Figure 8 shows TA102 with all three nanoparticles; clearly, HNT and MWCNT may have potential for a toxicity effect on this strain. Both TA1537 and TA1538 showed no significant toxic trends with the three nanoparticles (Figures 9 and 10).

### *Toxicity Testing: LB Broths*

The LB toxicity tests (broth tests) demonstrated a varied response to the nanoparticles. The *Escherichia coli* BW25113 showed decreasing trends in cell growth when compared to the control for the following treatments: Cloisite® dark/aerobic; HNT dark/aerobic; HNT dark/anaerobic; and MWCNT dark/anaerobic (Figure 11).

Importantly, this strain showed decreased cell growth only under both dark conditions.

The *E. coli* BW25113 *oxyR* mutant, when compared to *E. coli* BW24113, had overall more decreased growth trends; however, this strain showed effects under completely different treatments when compared to the wildtype (Figure 12). More decreases in growth were seen under light conditions for the *E. coli* BW25113 *oxyR* strain rather than dark conditions. Treatments with decreased growth included: all four treatments under Cloisite® conditions, both light treatments under HNT conditions, and finally both light treatments and the dark aerobic treatment under MWCNT conditions.

The *E. coli oxyR/pCA24N* strain showed statistically significant cell growth decreases under all anaerobic conditions for all three nanoparticles (Figure 13). When compared to the wildtype, this strain was affected more severely. This strain also showed increased cell growth under both aerobic Cloisite® conditions, specifically when exposed to the highest concentration of the Cloisite® nanoparticle. Importantly, this strain showed strong potential toxicity trends under all anaerobic treatments.

The *E. coli oxyR/pCA24N-oxyR* strain showed numerous potential toxic trends (Figure 14). For the Cloisite® and HNT treatments, both of the dark conditions had decreased cell growth as well as the HNT light aerobic treatment. Three of the four

MWCNT treatments showed decreased cell growth: both of the dark conditions and the light anaerobic condition.

*Escherichia coli* MG1655 also showed statistically significant changes in growth when exposed to the nanoparticles (Figure 15). Under both of the Cloisite® anaerobic conditions there were significant decreases in growth. Under all four MWCNT treatments, significant decreases in cell growth occurred as well. However, under some of the HNT conditions (light/aerobic, light/anaerobic, and dark/anaerobic), both the  $10^{-1}$  g and  $10^{-10}$  g treatments showed significant increases in cell growth when compared to the control.

*E. coli* ZK1000 had decreased growth with the Cloisite® treatments as well as the HNT treatments (Figure 16). However, for the MWCNT treatments, only under the dark conditions were any effects seen. Overall, this strain showed decreased growth with all three nanoparticles. With two treatments, the Cloisite® dark/aerobic  $10^{-1}$  g and the HNT light/aerobic  $10^{-15}$  g, statistically significant increased growth was seen.

All three Ames strains (TA102, TA1537, and TA1538) illustrated diverse effects towards the nanoparticles (Figures 17-19). All tests showed bacteria performance decreasing in the presence of MWCNTs. TA102 showed that the MWCNT hindered cell growth in the absence of light under both aerobic and anaerobic conditions. TA1537 showed with the Cloisite® under light conditions there was significant increased growth. The HNT treatments saw decreases in growth under dark conditions, while with light conditions, growth increased. The MWCNT had decreased growth under dark conditions (both aerobic and anaerobic) while with light conditions increased growth was seen. TA1538 had no significant changes for either Cloisite® or HNT treatments. Statistically,

the bacteria performed the same in the tests as in the controls. For the MWCNT tests, under dark conditions, there were significant effects seen when compared to the control. Under anaerobic conditions, cell growth decreased in the presence of the MWCNT. In light conditions, three of the MWCNT treatments saw decreased cell growth, while one treatment showed enhanced growth, possibly signifying mutagenic effects.

*Salmonella typhimurium* LT-2 strain showed under both aerobic conditions that potential toxic trends were observed in the presence of all three nanoparticles (one exception being Cloisite® aerobic/light, where growth increased, Figure 20). More toxic trends were observed under light conditions rather than dark conditions for this strain.

The two *Salmonella* mutant strains demonstrated less growth than the parent strain, *S. typhimurium* LT-2. The *S. typhimurium* SGSC 1336 *oxyR*- strain, when compared to the wildtype and the *S. typhimurium* SGSC 2618 *rpoS*- mutant, performed the worst (Figure 21). Every treatment of nanoparticles showed significant negative effects on *S. typhimurium oxyR*-. For the *S. typhimurium* SGSC 2618 *rpoS*- strain, all three nanoparticles showed negative trends (Figure 22). When compared to the wildtype, more toxic effects were seen under dark conditions. However, when compared to the *oxyR*- strain, the *rpoS*- mutant performed much better.

#### *Transmission Electron Microscopy*

Transmission electron microscope imaging (Figure 23) showed all three nanoparticles possibly attaching to *S. typhimurium* LT-2. Figure 23: A, C, and E shows images of the nanoparticles only, while Figure 23: B, D, and F display images of the bacteria in the presence of nanoparticles.

### *Growth Curves*

The *E. coli* BW25113 growth curve showed the Cloisite® nanoparticle as having the greatest negative effect on cell viability after 72 hours (Figure 24) while *E. coli oxyR* showed that the greatest loss of cell viability occurred under the MWCNT treatment (Figure 25). For strains *E. coli oxyR/pCA24N*, *E. coli oxyR/pCA24N-oxyR*, *E. coli* MG1655, and *E. coli* ZK1000 cell viability decreased substantially in the presence of the MWCNT (Figures 26-29). *E. coli oxyR/pCA24N* began to see significant decreases around ten hours, while the *E. coli oxyR* strain showed significant decreases in cell growth around 30 hours. Both *E. coli* MG1655 and *E. coli* ZK1000 showed decreases in growth also around ten hours.

TA102 showed all three nanoparticle growth curves having growth curves with values less than the LB control, (Figure 30); while TA1537 showed the MWCNT decreasing cell viability around ten hours (Figure 31). TA1538 showed the MWCNT decreasing cell growth at 15 hours (Figure 32). For all Ames strains, the two clay nanoparticles had growth curves very similar to the LB control growth curves.

*Salmonella typhimurium* LT-2 showed all three nanoparticle growth curves having values less than the control, especially the MWCNT growth curve (Figure 33). *Salmonella typhimurium oxyR* also showed all three nanoparticles having decreased cell viability; however, the HNT growth curve showed the most significant decreased cell viability (Figure 34). *Salmonella typhimurium rpoS* showed that the MWCNTs affected this strain the most in the growth curve experiment (Figure 35). Interestingly, two strains performed better in the presence of a nanoparticle when compared to the control; TA1537

when exposed to HNT outperformed the control as well as did *E. coli* MG1655 when also exposed to HNT.

## DISCUSSION

### *Ames Test*

For the Ames test to be considered significant, each treatment of the potential mutagenic compound must yield double the amount colonies when compared to the negative control. Only one Ames treatment gave close results; *Salmonella typhimurium* TA102 tested with the Cloisite® showed potential mutagenic effects; the amount of colonies was not quite double the control. TA102 also showed that HNT has no mutagenic effect, but rather a potential toxic trend was seen, while the MWCNT has a neutral effect (Figure 5). TA1537 showed the Cloisite and MWCNT to have a weak potential towards a mutagenic trend; the CFUs of the treatments are increased slightly when compared to the control; however, the CFUs are not double that of the negative control and cannot be considered significant. The HNT shows the treatments having lower CFU values than the control, suggesting that HNT exhibits possible toxicity but not mutagenicity (Figure 6).

TA1538 showed the Cloisite® to have the potential for a weak mutagenic trend; but not a significant mutagenic trend. Additionally, the HNT and MWCNT have a potential toxic trend; the CFU values for the treatments are lower when compared to the controls (Figure 7). Also, potential toxic trends were seen with the Ames test; TA1538 under HNT and MWCNT conditions had less growth when compared to the control. These two nanoparticles showed inhibition of TA1538 growth. Overall, the Ames test confirmed that while the nanoparticles may have very small mutagenic effects, the results

here were not significant or conclusive as to whether the nanoparticles caused such effects. Furthermore, it appeared as though the nanoparticles could exhibit potential toxic trends rather than true mutagenic trends.

#### *Toxicity Testing: LB Plates*

The LB toxicity tests (plates) show different results than the Ames tests. TA102 in the presence of HNT and MWCNTs shows potential for a slight toxicity trend (Figure 8). The Cloisite® nanoparticle seems to have no net effect on TA102; in fact all treatments show a similar trend when compared to the control. Contrastingly, the Ames test showed the Cloisite® to have a potential mutagenic effect at higher nanoparticle concentrations on TA102. However, with the LB toxicity plates we see no significant effect for the Cloisite®.

With TA1537, it appears that all three nanoparticles have no significant toxic effect (Figure 9). For the Ames test on TA1537, we saw slight effects on the strain in the presence of the Cloisite® and MWCNT. TA1538 showed no significant toxic results for the LB tests when treatments are compared to the controls (Figure 10). However, for the Ames test on TA1538, we did see a potential toxic trend.

#### *Toxicity Testing: LB Broths*

The LB toxicity tests (broths) showed a variety of responses including some increased cell growth, possibly indicating the nanoparticles could have beneficial properties (Figures 11-22). For *Escherichia coli* BW25113 (wt), statistically significant decreases in growth were seen under only dark conditions (Figure 11). The *E. coli* BW25113 *oxyR* strain, had more significant decreases in cell growth when compared to the wildtype (Figure 12); however under different treatments. This knockout mutant was

affected the most out of the three *E. coli* mutants used in this study (*E. coli* BW25113 *oxyR*, *E. coli oxyR/pCA24N*, and *E. coli oxyR/pCA24N-oxyR*). Considering that the *E. coli* BW25113 *oxyR* strain is lacking a functional *oxyR* gene (7, 10, 15, 24), the results seen for the LB toxicity broth tests coincide with that was expected. Due to its nonfunctional gene, the *E. coli* BW25113 *oxyR* strain cannot effectively protect itself from oxidative stresses (7, 10, 15, 24). The *E. coli* BW25113 *oxyR* strain showed decreased growth among the following treatments: all four Cloisite® tests, both light tests for the HNT, and both light tests as well as the dark aerobic test for the MWCNT.

*Escherichia coli oxyR/pCA24N* showed significant decreases in cell growth under all anaerobic conditions for all three nanoparticles (Figure 13). Again, when compared to the wildtype, this strain had more significant decreases in cell growth, due to it lacking the *oxyR* gene. However; when compared to the strain *E. coli oxyR/pCA24N-oxyR*, the *E. coli oxyR/pCA24N* strain performed slightly better. This is interesting as the *E. coli oxyR/pCA24N-oxyR* strain has a functional *oxyR* gene incorporated into the plasmid and should be able to combat oxidative stresses (7, 10, 15, 24). The *E. coli oxyR/pCA24N-oxyR* strain is highly susceptible to all three nanoparticles (Figure 14). When compared to the wildtype, *E. coli oxyR/pCA24N-oxyR* overall had more significant decreases in cell growth, especially in three tests: the HNT light/aerobic test, the MWCNT light/anaerobic test, and the Cloisite® dark/anaerobic test. This strain should have performed similarly to the wildtype strain, as they both contain functional *oxyR* genes.

For strain *E. coli* MG1655, again there were potential toxic trends seen among nanoparticle treatments (Figure 15). However, here cell growth also increased under some of the HNT treatments. In environmental conditions, when this strain is exposed to

halloysite clays, beneficial impacts may happen as clays have the ability to exchange ions with the environment. Bacteria can interact with these ions by donating a proton to the clay and seizing the now free ion. This interaction may be reflected in the exceptional growth patterns of this strain when exposed to the clay in the toxicity tests.

The *E. coli* ZK1000 strain also showed overall toxic trends with all three nanoparticles (Figure 16). Interestingly, this strain, like *E. coli* MG1655, showed increased growth under one of the Cloisite® and one of the HNT treatments. Again, these two nanoparticles are clays and could have significant impacts with growth of bacterial communities in environmental settings. The *E. coli* ZK1000 strain is missing its *rpoS* gene and the toxicity trends for *E. coli* ZK1000 could be due to the absent gene not combating oxidative stresses brought on by the nanoparticles. When compared to *E. coli* strains MG1655 and BW25113, *E. coli* ZK1000 overall performs much worse across all treatments. This again, may be due to the missing *rpoS*- gene that the other two *E. coli* strains contain.

The Ames strains showed varied results under the LB toxicity broth tests. TA102 shows that the MWCNT has a toxic trend (Figure 17). TA1537 under light conditions, showed each nanoparticle having the potential for slight mutagenesis, while under dark conditions; the three nanoparticles appeared to have potential toxic trends (Figure 18). TA1538 showed that the Cloisite® and HNT nanoparticles do not have a mutagenic or toxic effect, but rather that the MWCNT does have potential toxic effects, and in one case, may have potential mutagenic effects (MWCNT dark/aerobic condition, Figure 19).

The two knockout *S. typhimurium* strains did comparatively worse when compared to their wildtype (Figures 20-22). This signifies that both the *rpoS*- and *oxyR*-

genes may be crucial to combating oxidative stresses caused by nanoparticles.

Importantly, it appears that the *oxyR* gene is more crucial for bacterial survival than the *rpoS* gene. This can be evaluated through the severe toxic trends seen on the *S. typhimurium* SGSC 1336 *oxyR* strain when compared to *S. typhimurium* SGSC 2618 *rpoS*.

### *Growth Curves*

All 12 strains were grown in the presence of the three nanoparticles as well as LB, which served as the control. Eleven of the 12 strains showed some decrease in growth when grown in the MWCNT when compared to the LB control. Five of the 12 strains showed exceptional decreases in growth, these included: *E. coli* MG1655, *E. coli* ZK1000, *S. typhimurium* TA102, TA1537, TA1538, and *S. typhimurium* LT-2. One strain, *E. coli* BW25113 (wt) showed decreased in growth when grown with the Cloisite® nanoparticle when compared to the LB control (Figure 25). *Salmonella typhimurium* SCSG 1336 *oxyR* showed decreased growth under HNT conditions (Figure 34). Finally, two strains, TA1537 and *E. coli* MG1655 showed increased growth in the presence of HNT when compared to the control. For these strains, the halloysite nanoparticle had beneficial effects, helping them to outgrow even the control.

### *Conclusions*

One possible deficiency of the Ames test is due to the assay not being performed in a mixed culture. In true environmental conditions, bacteria are not found as a pure culture; in fact, it is believed that 1 g of soil may contain up to one million different types of microbes (54). Therefore, it may be more relevant to design a unique derivative of the Ames test that deals with mixed culture. Also, bacteria are not adequately exposed to the

mutagens when in an agar environment. More conclusive evidence may be seen in a liquid environment where bacteria can be constantly exposed to the mutagens. This also applies to the LB toxicity plate tests; bacteria may not receive sufficient exposure to the toxic compounds to see a true toxic effect. Again, a liquid test can demonstrate more accurate effects because bacteria can constantly interact with the toxic compounds.

Toxicity is not a general effect across bacterial species (that were tested in this study). In fact, *Salmonella* was affected more than *Escherichia* as seen by the strain *S. typhimurium oxyR*. The MWCNT affected the *S. typhimurium* SGSC 1336 *oxyR* significantly. It appears that the *oxyR* gene is more important for combating oxidative stress caused by nanoparticles rather than the *rpoS* gene (when compared to the *S. typhimurium* SGSC 2618 *rpoS*) for *Salmonella* species. For *E. coli*, the effects of the nanoparticles are not as dramatic when compared to the *Salmonella* strains. The *E. coli* BW25113 *oxyR* strain exhibited much less negative effects when compared to the *S. typhimurium* SGSC 1336 *oxyR*. To accurately determine if *oxyR* is an important gene for *Salmonella* survival in the presence of nanoparticles, a complemented *oxyR* strain should be utilized for additional work. With the two clay nanoparticles, trends varied greatly and no general toxicity effect was observed. With the MWCNT, potential toxicity trends were seen amongst numerous strains.

#### *Closing Remarks*

Future work with bacteria and nanoparticles could be extrapolated to include biofilm, algal, protozoan, and fungal research. It may be possible that biofilms are less likely to see strong toxic effects when encountering nanoparticles, unlike their planktonic counterparts. This research could also include work with mixed cultures. Communities

of bacteria may be able to resist effects of nanoparticles more thoroughly than single species communities. Future research in these areas is crucial to understanding how bacterial communities are affected; indeed, biofilms could one day even play a role in nanoparticle remediation.

Also, possible synergistic effects of nanoparticles should be studied. One species of bacteria or even a bacterial community may behave differently if it is exposed to a community of nanoparticles rather than just a single type of nanoparticle. Notably, this research will have important implications on managing the disposal of nanoparticles. If copious amounts of nanoparticles reach our watersheds and interact with other compounds, the consequences would be wide reaching and diverse. It may also be important to study nanoparticles under other conditions, such as temperature effects, interactions with nutrients in aquatic systems, influences on organic matter breakdown, UV light exposure, and finally contact with other compounds such as herbicides and pesticides. Current nanotechnology research will hopefully give answers to many of the pressing questions at hand, from exposure and human health, to nanoparticle delivery of medicines.

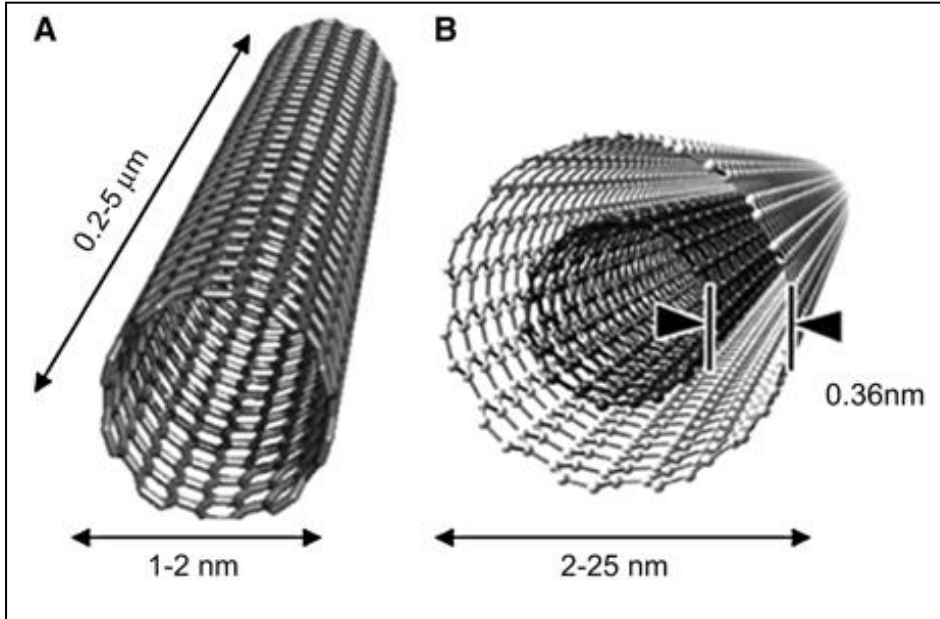


**Figure 1: Carbon nanotube structure.** Conceptual diagram of single-walled carbon nanotube (SWCNT) (A) and multi-walled carbon nanotube (MWCNT) (B) showing typical dimensions of length, width, and separation distance between graphene layers in MWCNTs (47).

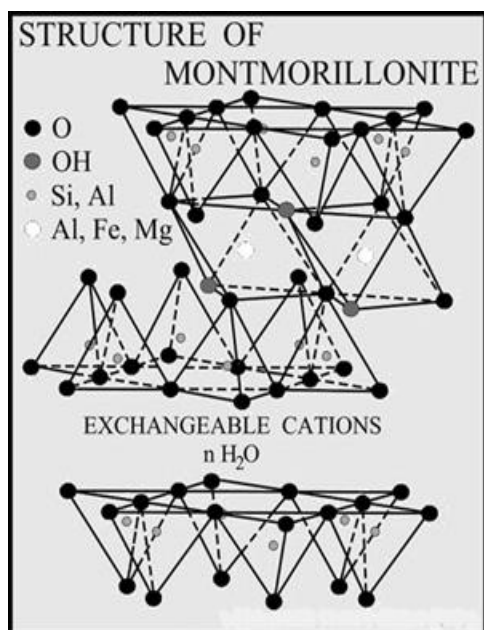


Figure 2: Montmorillonite clay structure (57).

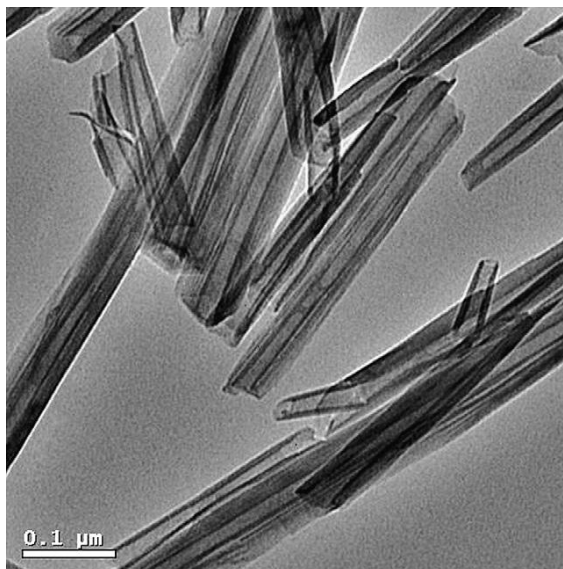


Figure 3: Transmission electron microscope image of halloysite nanotubes (31).

**Table 1: Organisms used as inoculum species.**

Strain	Genotype	Media	Antibiotic Requirements	Source
<i>Escherichia coli</i> BW25113	wildtype	LB	-	T.K. Wood (Texas A&M)
<i>E. coli</i> BW25113 <i>oxyR</i>	<i>oxyR</i> mutant	LB	kanamycin 50 µg/mL	T.K. Wood (Texas A&M)
<i>E. coli</i> BW25113 <i>oxyR</i> /pCA24N	plasmid without <i>oxyR</i> gene	LB	kanamycin 50 µg/mL and chloramphenicol 30 µg/mL	T.K. Wood (Texas A&M)
<i>E. coli</i> BW25113 <i>oxyR</i> /pCA24N- <i>oxyR</i>	plasmid with <i>oxyR</i> gene	LB	kanamycin 50 µg/mL and chloramphenicol 30 µg/mL	T.K. Wood (Texas A&M)
<i>E. coli</i> ZK1000	<i>rpoS</i> mutant	LB	-	(7)
<i>E. coli</i> MG1655	wildtype	LB	-	ATCC# 47076
<i>Salmonella typhimurium</i> SGSC 1336	<i>oxyR</i> mutant	LB	kanamycin 50 µg/mL	K.E. Sanderson (University of Calgary)
<i>S. typhimurium</i> SGSC 2618	<i>rpoS</i> mutant	LB	ampicillin 100 µg/mL	K.E. Sanderson (University of Calgary)
<i>S. typhimurium</i> LT-2	wildtype	LB	-	C.A. Nickerson (Arizona State University)
<i>S. typhimurium</i> TA102	Ames Strain	NB	ampicillin 25 µg/mL and tetracycline 2 µg/mL	B. Ames (Berkeley)
<i>S. typhimurium</i> TA1538	Ames Strain	NB	-	B. Ames (Berkeley)
<i>S. typhimurium</i> TA1537	Ames Strain	NB	-	B. Ames (Berkeley)

**Table 2: Davis minimal media recipe.**

Potassium phosphate (dibasic trihydrate)	7 g
Potassium phosphate (monobasic anhydrous)	2 g
Ammonium sulfate	1 g
Sodium citrate	0.5 g
Millipore Water	1000 mL
Agar	15 g
Glucose	4 g
Magnesium sulfate (10%)	1 mL
Thiamine (0.2%)	1 mL

**Table 3: LB broth toxicity test requirements for tests, controls, and blanks.**

Components	Test	Control	Blank
LB Liquid Media	4.5 mL	4.5 mL	4.5 mL
Nanoparticle Dilution	0.5 mL	0.5 mL	-
Bacteria (0.3 OD)	25 $\mu$ L	-	-
Anaerobic Conditions	1.0 mL Mineral Oil	-	-
Aerobic Conditions	-	-	-

**Table 4: Concentrations of nanoparticles used in the LB broth toxicity tests.**

Nanoparticle*	High Concentration	Medium-High Concentration	Medium-Low Concentration	Low Concentration
MWCNT	0.1 g	$1 \times 10^{-5}$ g	$1 \times 10^{-10}$ g	$1 \times 10^{-15}$ g
HNT	0.1 g	$1 \times 10^{-5}$ g	$1 \times 10^{-10}$ g	$1 \times 10^{-15}$ g
Cloisite®	0.1 g	$1 \times 10^{-5}$ g	$1 \times 10^{-10}$ g	$1 \times 10^{-15}$ g

\*Each test had three replicates of each concentration of nanoparticles as well as three aerobic and three anaerobic controls, which contained no nanoparticles.

**Figure 4: LB toxicity tests under light conditions.**

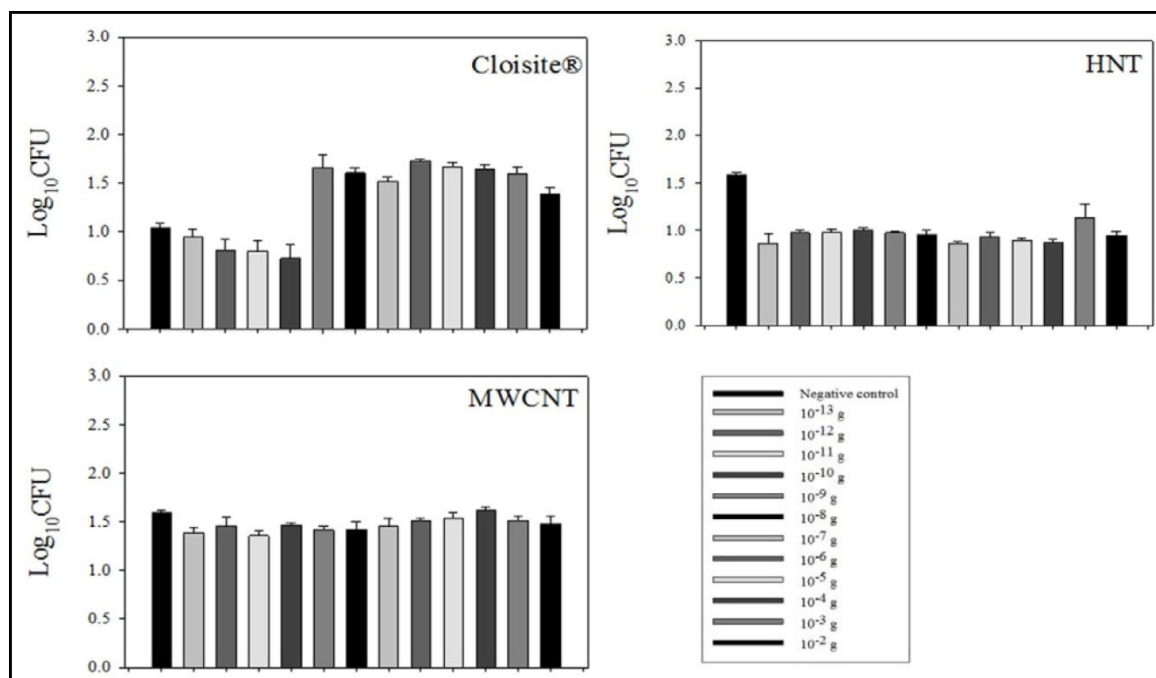


**Figure 5:** Ames test *S. typhimurium* TA102. The negative control contains no nanoparticles, only Davis Minima media and the appropriate bacteria (bacteria plated at 0.3 OD<sup>600</sup>). 10<sup>-13</sup> g to 10<sup>-2</sup> g corresponds to exposure of the bacteria to varying concentrations of nanoparticles.

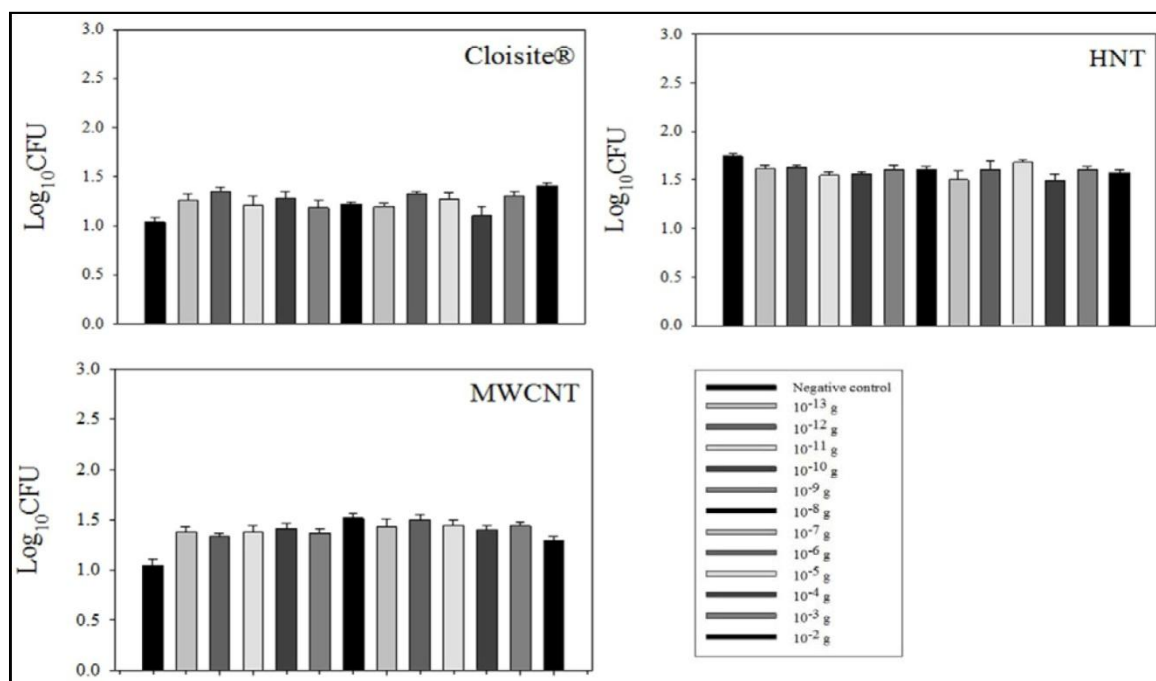


**Figure 6:** Ames test *S. typhimurium* TA1537. The negative control contains no nanoparticles, only Davis Minima media and the appropriate bacteria (bacteria plated at 0.3 OD<sup>600</sup>). 10<sup>-13</sup> g to 10<sup>-2</sup> g corresponds to exposure of the bacteria to varying concentrations of nanoparticles.

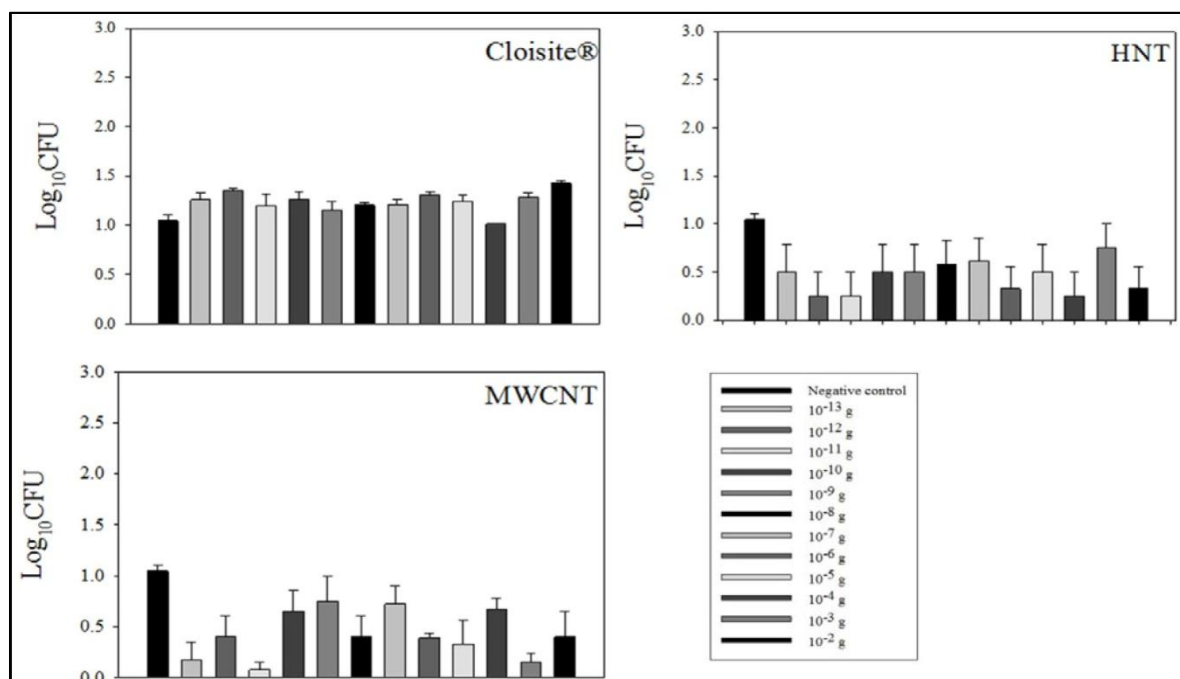


**Figure 7: Ames test *S. typhimurium* TA1538.** The negative control contains no nanoparticles, only Davis Minimal media and the appropriate bacteria (bacteria plated at  $0.3 \text{ OD}^{600}$ ).  $10^{-13}$  g to  $10^{-2}$  g corresponds to exposure of the bacteria to varying concentrations of nanoparticles.

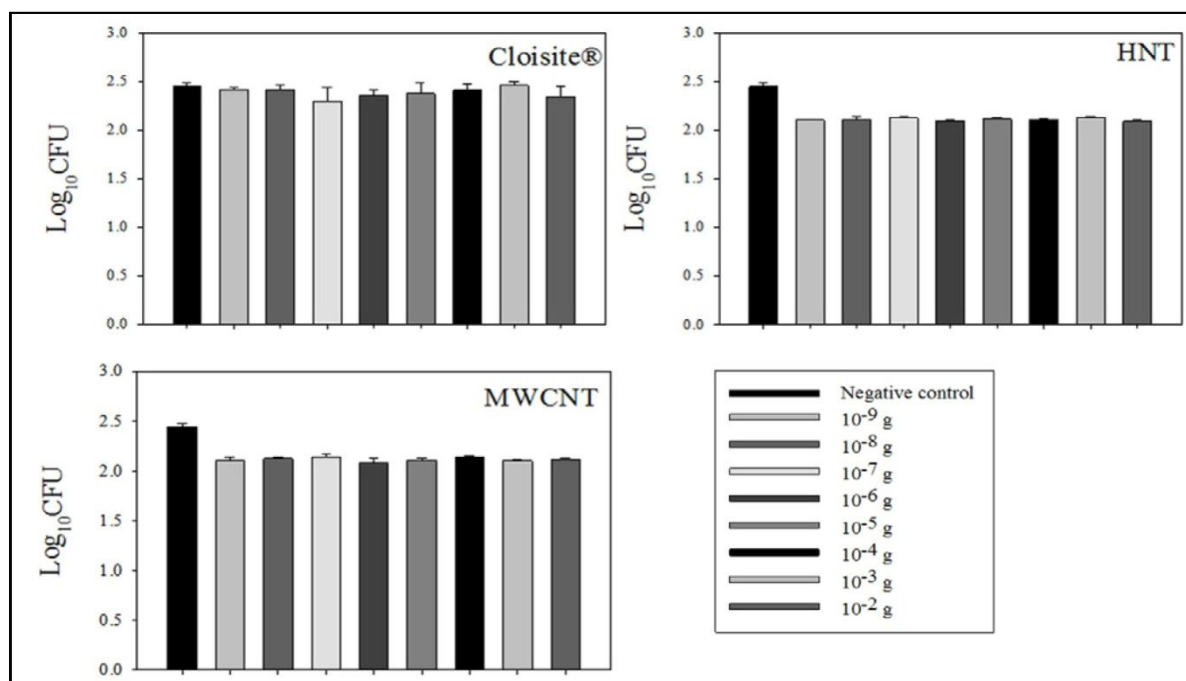


**Figure 8: LB toxicity test (plate) *S. typhimurium* TA102.** The negative control contains no nanoparticles, only LB media and the appropriate bacteria (bacteria plated at  $0.3 \text{ OD}^{600}$ ).  $10^{-9}$  g to  $10^{-2}$  g corresponds to exposure of the bacteria to varying concentrations of nanoparticles.

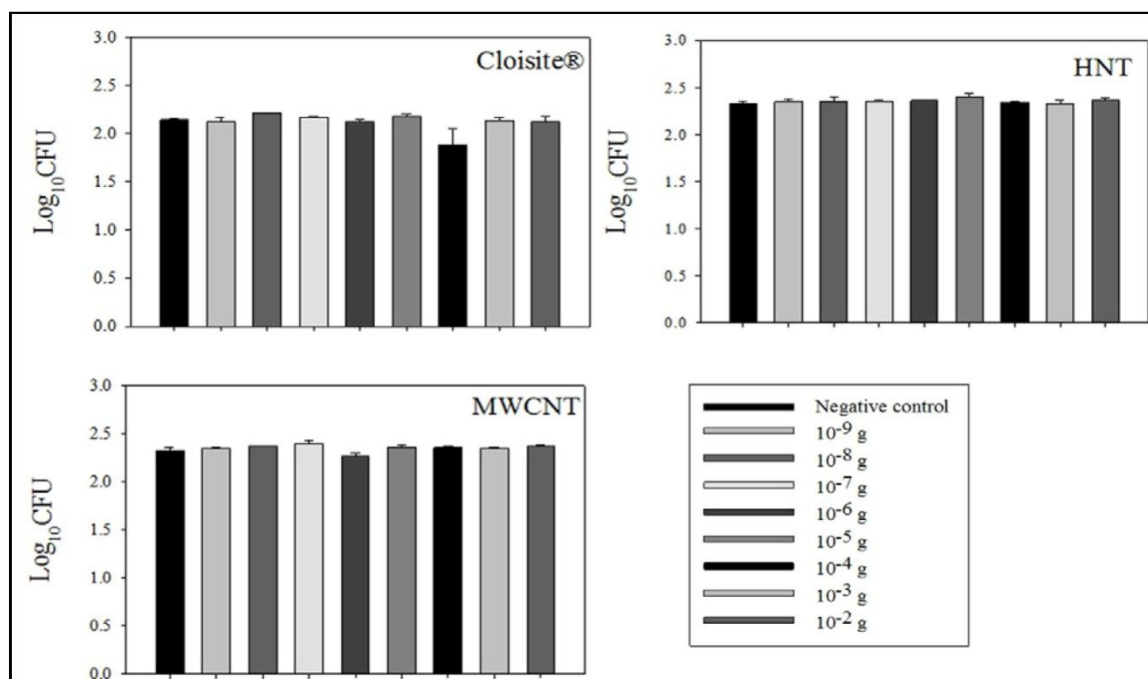


**Figure 9: LB toxicity test (plate) *S. typhimurium* TA1537.** The negative control contains no nanoparticles, only LB media and the appropriate bacteria (bacteria plated at 0.3 OD<sup>600</sup>). 10<sup>-9</sup> g to 10<sup>-2</sup> g corresponds to exposure of the bacteria to varying concentrations of nanoparticles.

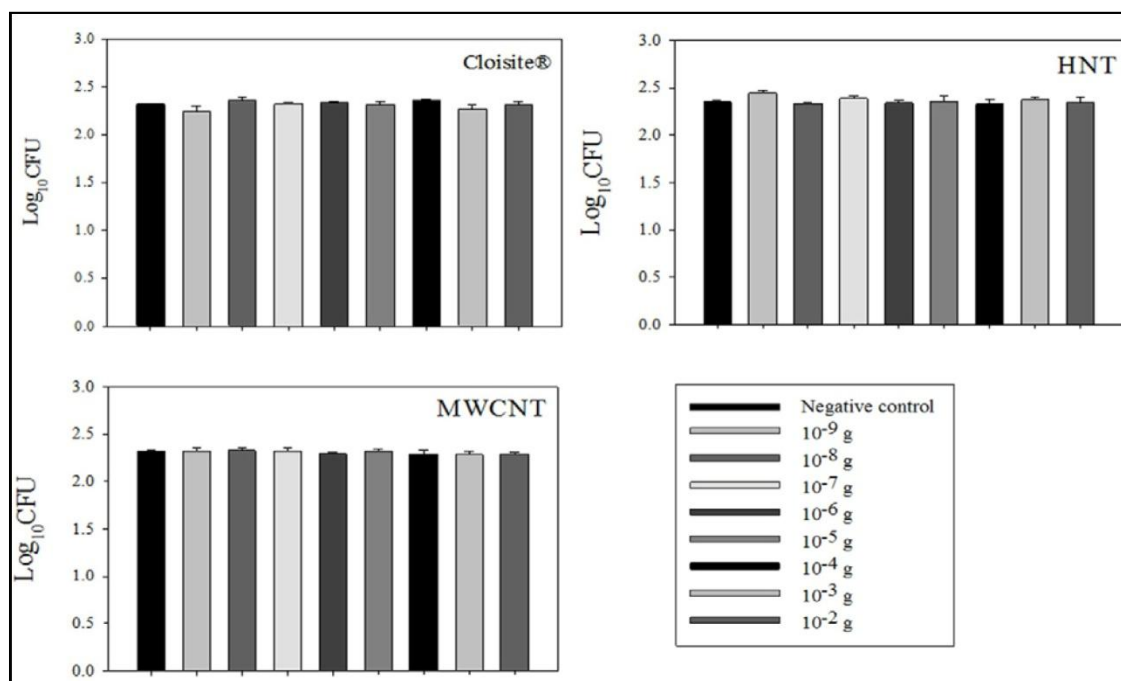


**Figure 10: LB toxicity test (plate) *S. typhimurium* TA1538.** The negative control contains no nanoparticles, only LB media and the appropriate bacteria (bacteria plated at 0.3 OD<sup>600</sup>). 10<sup>-9</sup> g to 10<sup>-2</sup> g corresponds to exposure of the bacteria to varying concentrations of nanoparticles.

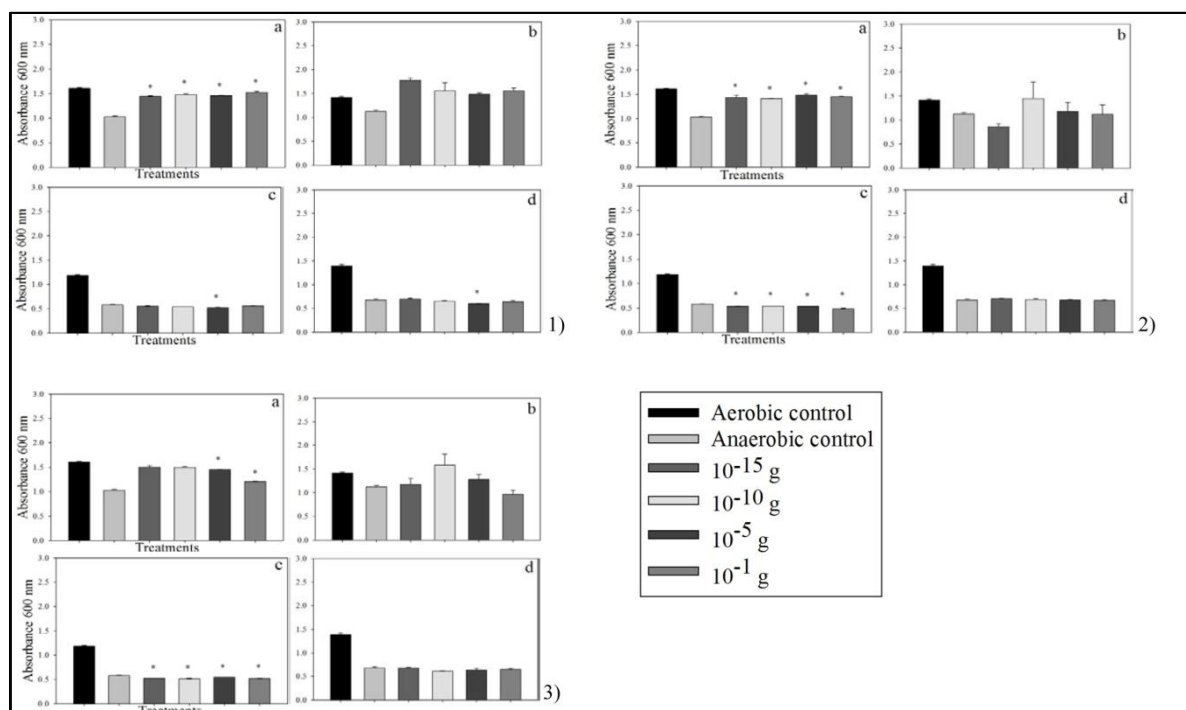


**Figure 11: LB toxicity (broth) test *E. coli* BW25113.** Strains were evaluated under varying conditions: a) dark and aerobic, b) light and aerobic, c) dark and anaerobic, and d) light and anaerobic. The Kruskal-Wallis One Way Analysis of Variance on Ranks (non-parametric ANOVA) was performed to indicate significance among different groups. The \* indicates significance with the Holm-Sidak t- test ( $P < 0.05$ ) when treatments were compared to the appropriate control (aerobic treatments compared only to aerobic control and vice versa; the other control was used as a comparison only and was kept out of all statistical analysis). Data are presented as mean  $\pm$  S.E. 1 = Cloisite®, 2 = HNT, and 3 = MWCNT.

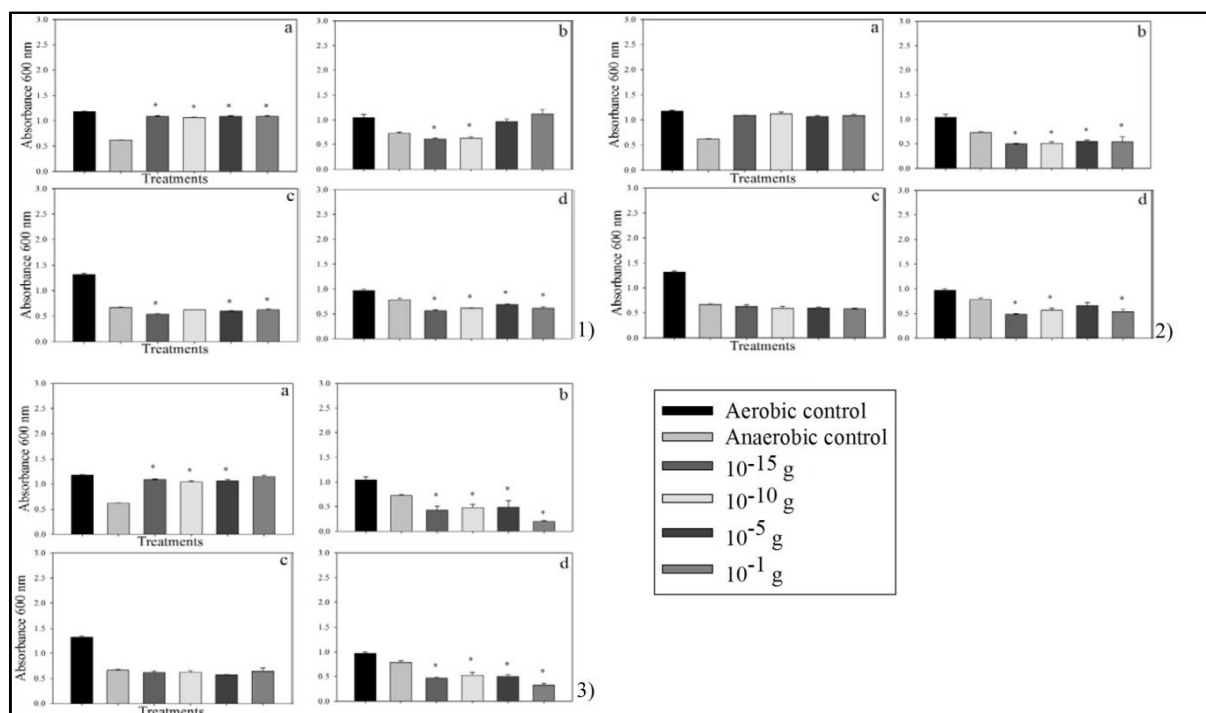


**Figure 12: LB toxicity (broth) test *E. coli* BW25113 *oxyR*.** Strains were evaluated under varying conditions: a) dark and aerobic, b) light and aerobic, c) dark and anaerobic, and d) light and anaerobic. The Kruskal-Wallis One Way Analysis of Variance on Ranks (non-parametric ANOVA) was performed to indicate significance among different groups. The \* indicates significance with the Holm-Sidak t- test ( $P < 0.05$ ) when treatments were compared to the appropriate control (aerobic treatments compared only to aerobic control and vice versa; the other control was used as a comparison only and was kept out of all statistical analysis). Data are presented as mean  $\pm$  S.E. 1 = Cloisite®, 2 = HNT, and 3 = MWCNT.

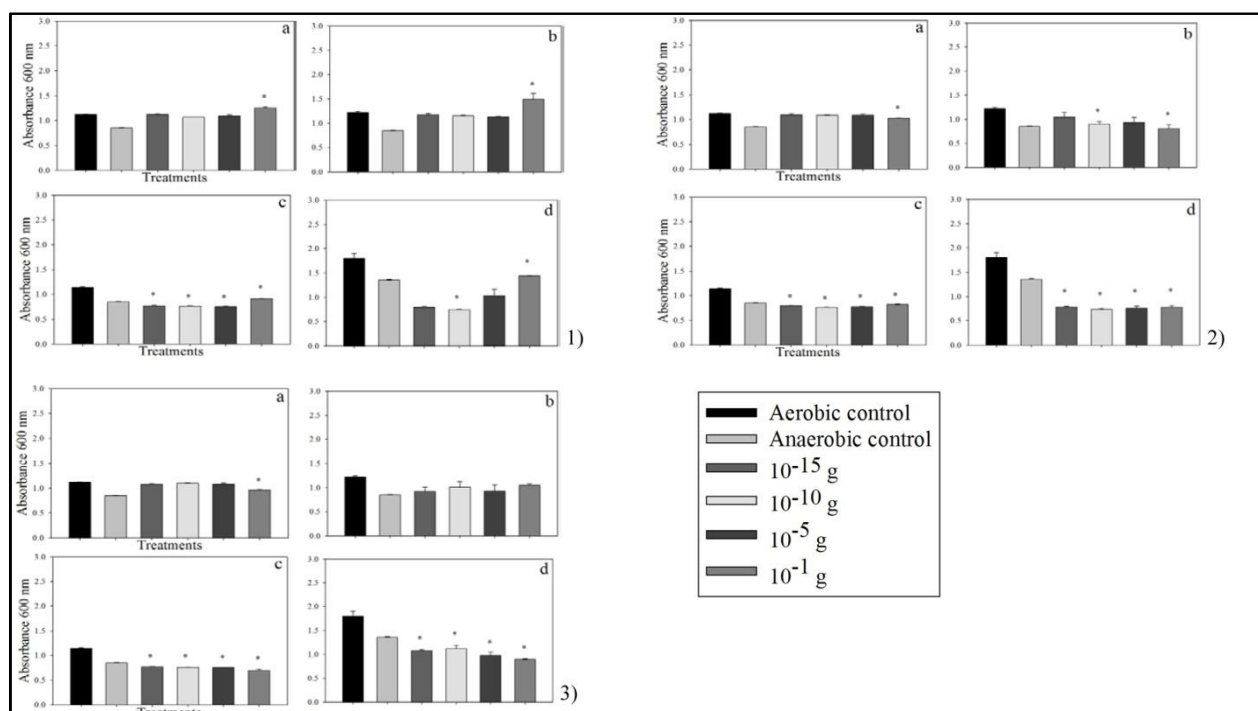


**Figure 13: LB toxicity (broth) test *E. coli oxyR/pCA24N*.** Strains were evaluated under varying conditions: a) dark and aerobic, b) light and aerobic, c) dark and anaerobic, and d) light and anaerobic. The Kruskal-Wallis One Way Analysis of Variance on Ranks (non-parametric ANOVA) was performed to indicate significance among different groups. The \* indicates significance with the Holm-Sidak t-test ( $P < 0.05$ ) when treatments were compared to the appropriate control (aerobic treatments compared only to aerobic control and vice versa; the other control was used as a comparison only and was kept out of all statistical analysis). Data are presented as mean  $\pm$  S.E. 1 = Cloisite®, 2 = HNT, and 3 = MWCNT.

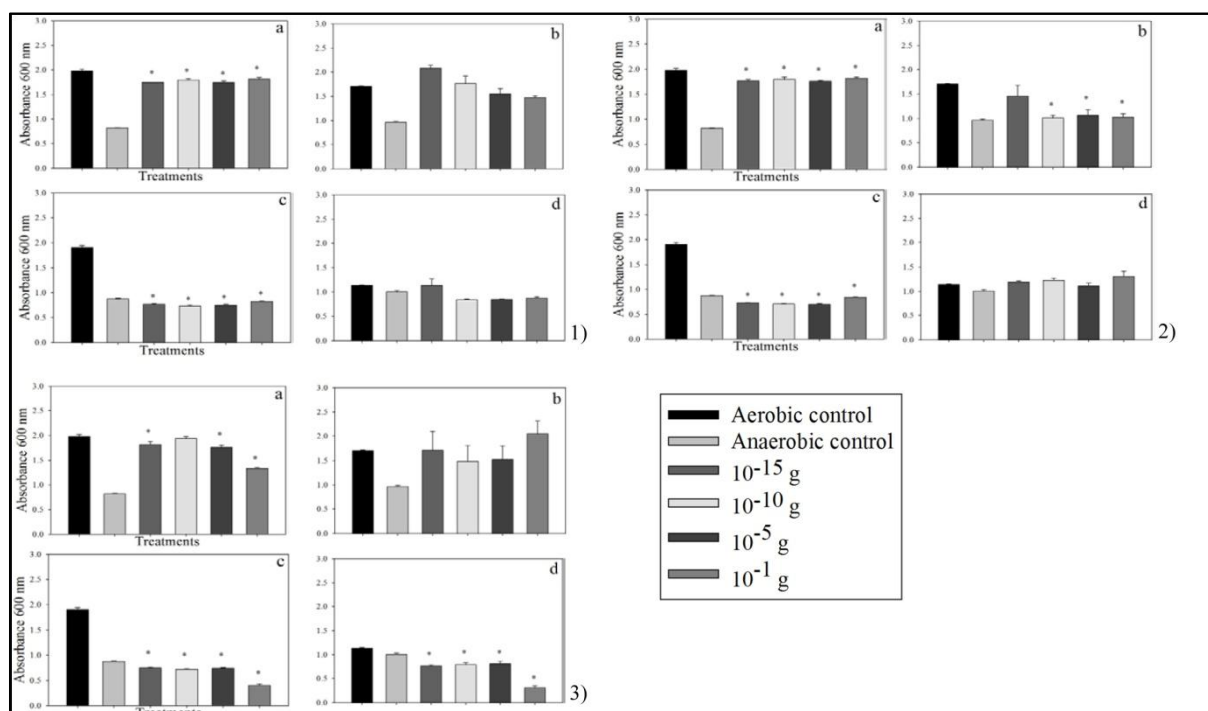


**Figure 14: LB toxicity (broth) test *E. coli* BW25113 *oxyR*/pCA24N-*oxyR*.** Strains were evaluated under varying conditions: a) dark and aerobic, b) light and aerobic, c) dark and anaerobic, and d) light and anaerobic. The Kruskal-Wallis One Way Analysis of Variance on Ranks (non-parametric ANOVA) was performed to indicate significance among different groups. The \* indicates significance with the Holm-Sidak t- test ( $P < 0.05$ ) when treatments were compared to the appropriate control (aerobic treatments compared only to aerobic control and vice versa; the other control was used as a comparison only and was kept out of all statistical analysis). Data are presented as mean  $\pm$  S.E. 1 = Cloisite®, 2 = HNT, and 3 = MWCNT.

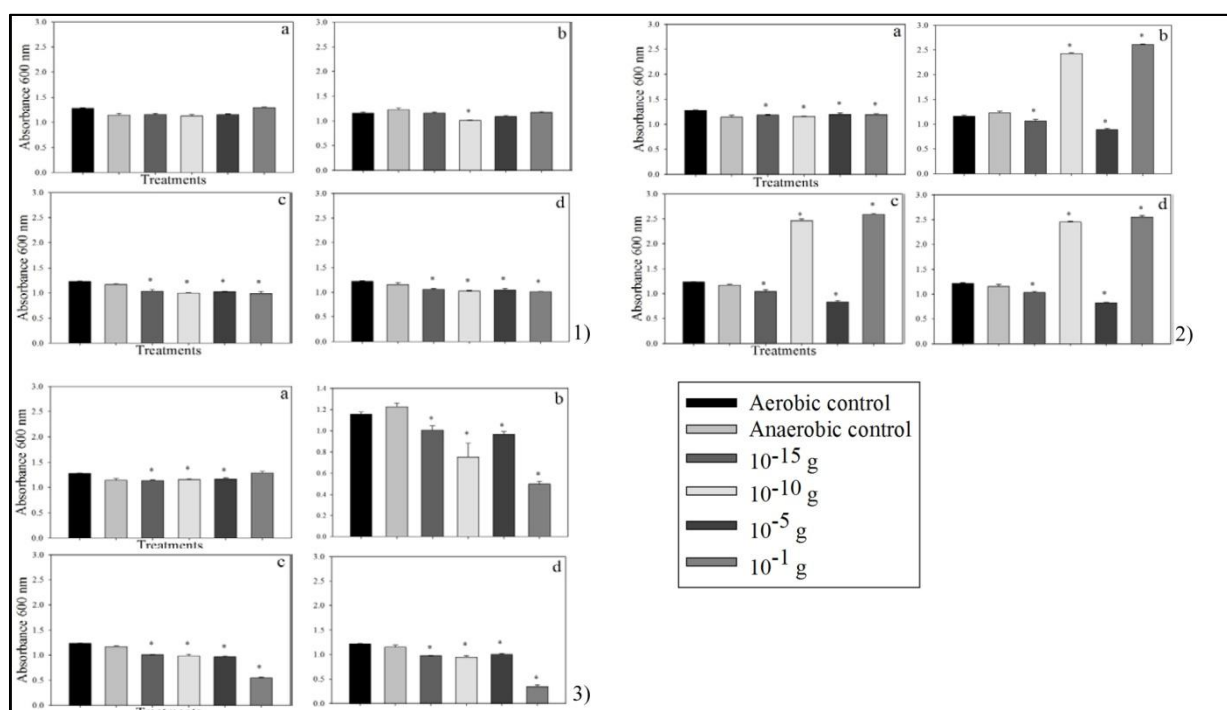


**Figure 15: LB toxicity (broth) test *E. coli* MG1655.** Strains were evaluated under varying conditions: a) dark and aerobic, b) light and aerobic, c) dark and anaerobic, and d) light and anaerobic. The Kruskal-Wallis One Way Analysis of Variance on Ranks (non-parametric ANOVA) was performed to indicate significance among different groups. The \* indicates significance with the Holm-Sidak t- test ( $P < 0.05$ ) when treatments were compared to the appropriate control (aerobic treatments compared only to aerobic control and vice versa; the other control was used as a comparison only and was kept out of all statistical analysis). Data are presented as mean  $\pm$  S.E. 1 = Cloisite®, 2 = HNT, and 3 = MWCNT.

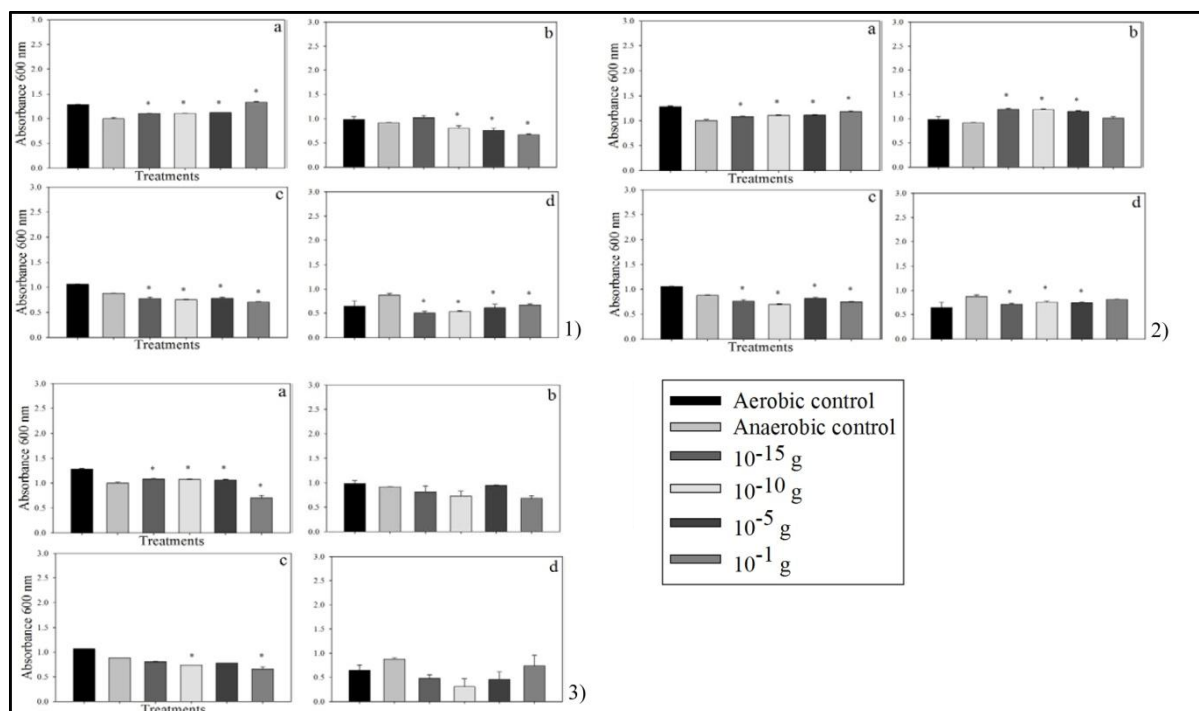


**Figure 16: LB toxicity (broth) test *E. coli* ZK1000.** Strains were evaluated under varying conditions: a) dark and aerobic, b) light and aerobic, c) dark and anaerobic, and d) light and anaerobic. The Kruskal-Wallis One Way Analysis of Variance on Ranks (non-parametric ANOVA) was performed to indicate significance among different groups. The \* indicates significance with the Holm-Sidak t- test ( $P < 0.05$ ) when treatments were compared to the appropriate control (aerobic treatments compared only to aerobic control and vice versa; the other control was used as a comparison only and was kept out of all statistical analysis). Data are presented as mean  $\pm$  S.E. 1 = Cloisite®, 2 = HNT, and 3 = MWCNT.

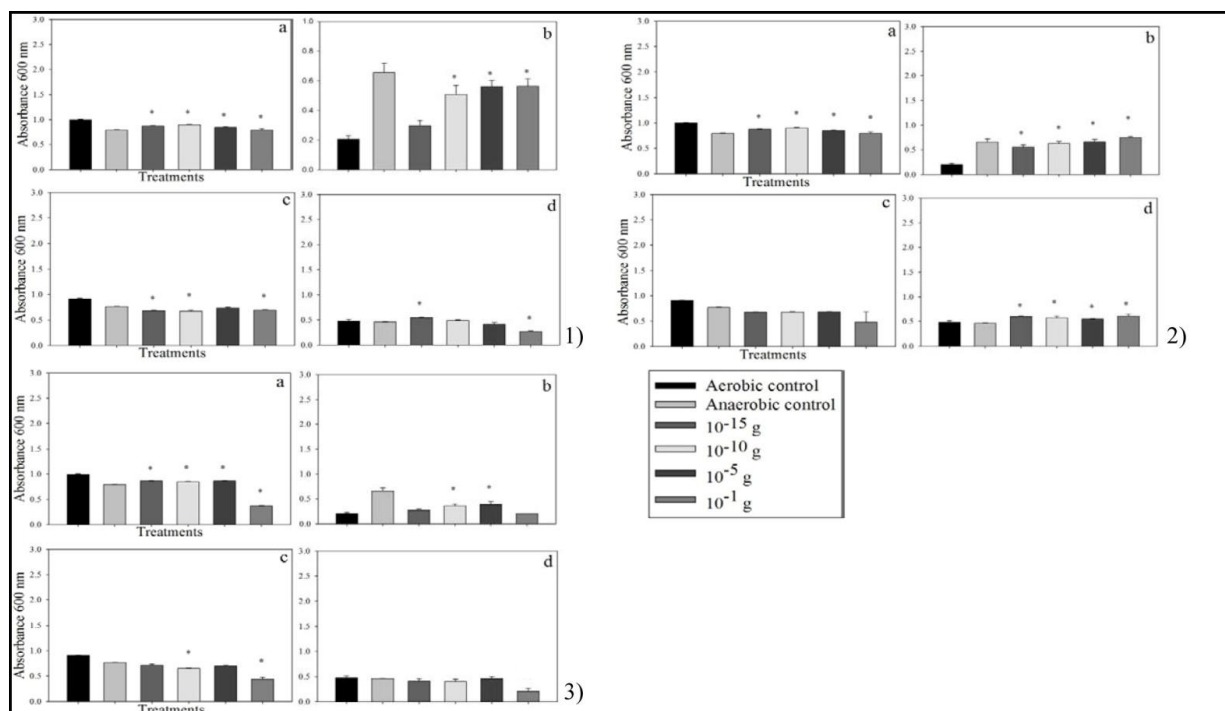


**Figure 17: LB toxicity (broth) test *S. typhimurium* TA102.** Strains were evaluated under varying conditions: a) dark and aerobic, b) light and aerobic, c) dark and anaerobic, and d) light and anaerobic. The Kruskal-Wallis One Way Analysis of Variance on Ranks (non-parametric ANOVA) was performed to indicate significance among different groups. The \* indicates significance with the Holm-Sidak t- test ( $P < 0.05$ ) when treatments were compared to the appropriate control (aerobic treatments compared only to aerobic control and vice versa; the other control was used as a comparison only and was kept out of all statistical analysis). Data are presented as mean  $\pm$  S.E. 1 = Cloisite®, 2 = HNT, and 3 = MWCNT.

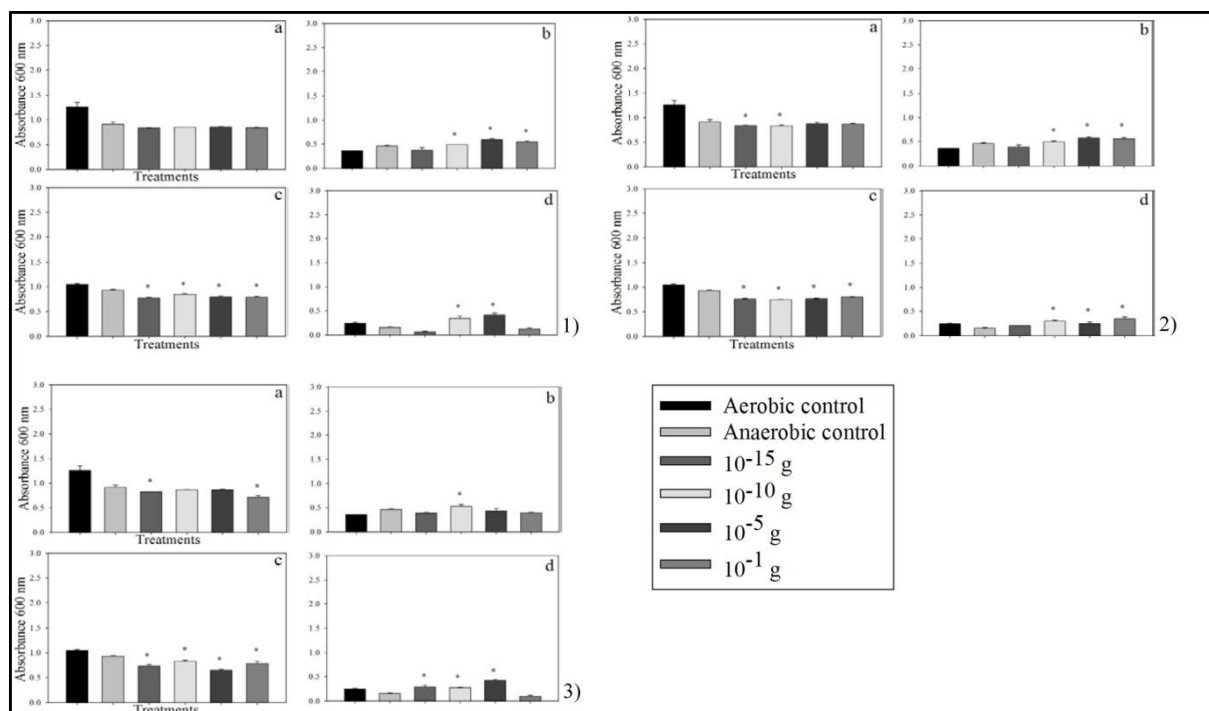


**Figure 18: LB toxicity (broth) test *S. typhimurium* TA1537.** Strains were evaluated under varying conditions: a) dark and aerobic, b) light and aerobic, c) dark and anaerobic, and d) light and anaerobic. The Kruskal-Wallis One Way Analysis of Variance on Ranks (non-parametric ANOVA) was performed to indicate significance among different groups. The \* indicates significance with the Holm-Sidak t- test ( $P < 0.05$ ) when treatments were compared to the appropriate control (aerobic treatments compared only to aerobic control and vice versa; the other control was used as a comparison only and was kept out of all statistical analysis). Data are presented as mean  $\pm$  S.E. 1 = Cloisite®, 2 = HNT, and 3 = MWCNT.

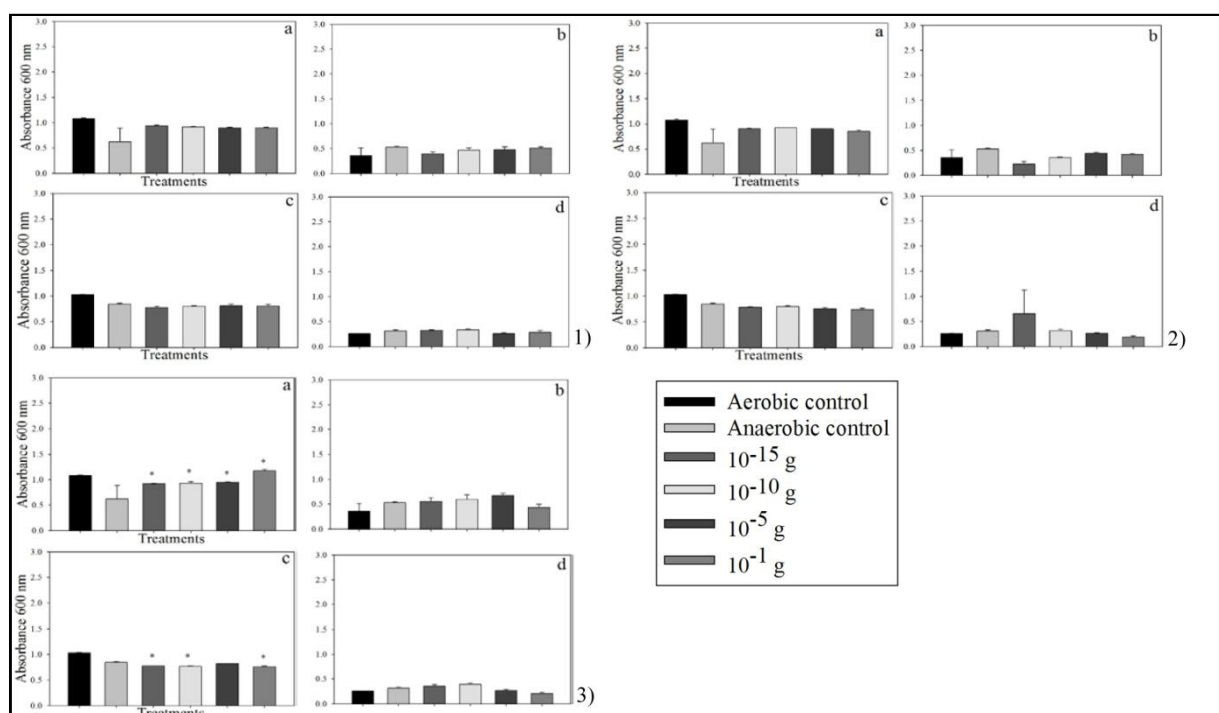


**Figure 19: LB toxicity (broth) test *S. typhimurium* TA1538.** Strains were evaluated under varying conditions: a) dark and aerobic, b) light and aerobic, c) dark and anaerobic, and d) light and anaerobic. The Kruskal-Wallis One Way Analysis of Variance on Ranks (non-parametric ANOVA) was performed to indicate significance among different groups. The \* indicates significance with the Holm-Sidak t- test ( $P < 0.05$ ) when treatments were compared to the appropriate control (aerobic treatments compared only to aerobic control and vice versa; the other control was used as a comparison only and was kept out of all statistical analysis). Data are presented as mean  $\pm$  S.E. 1 = Cloisite®, 2 = HNT, and 3 = MWCNT.

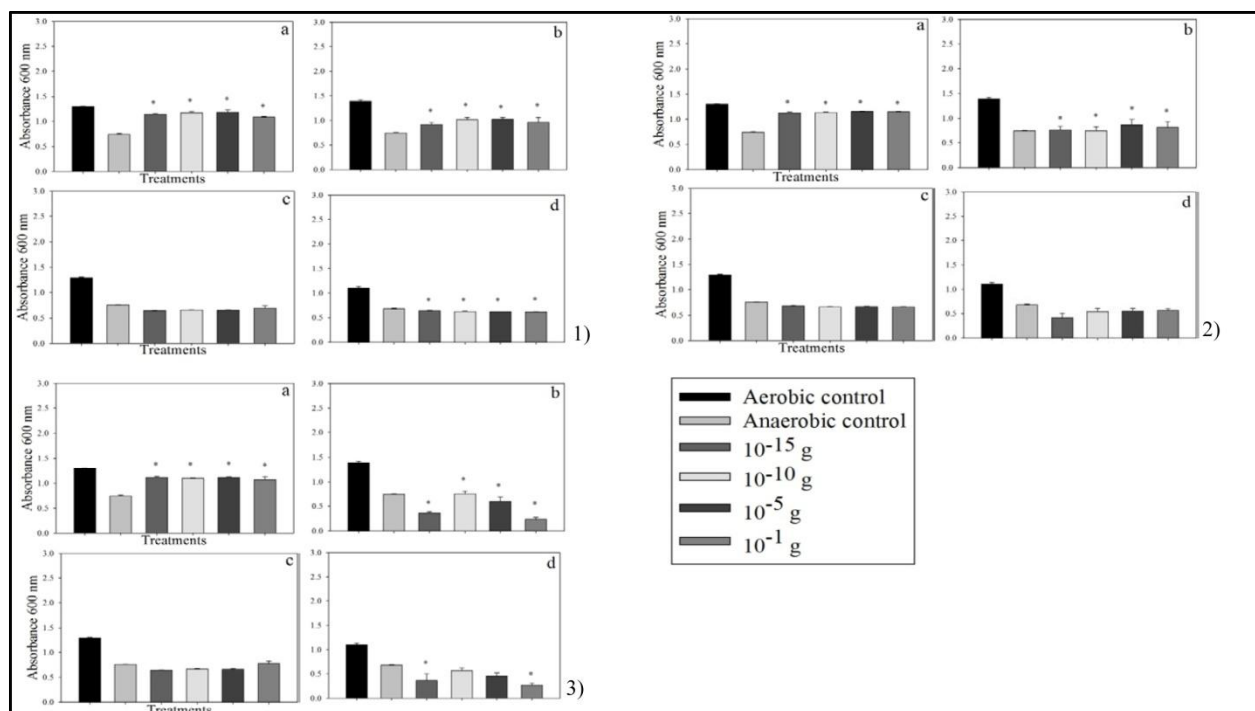


**Figure 20: LB toxicity (broth) test *S. typhimurium* LT-2.** Strains were evaluated under varying conditions: a) dark and aerobic, b) light and aerobic, c) dark and anaerobic, and d) light and anaerobic. The Kruskal-Wallis One Way Analysis of Variance on Ranks (non-parametric ANOVA) was performed to indicate significance among different groups. The \* indicates significance with the Holm-Sidak t- test ( $P < 0.05$ ) when treatments were compared to the appropriate control (aerobic treatments compared only to aerobic control and vice versa; the other control was used as a comparison only and was kept out of all statistical analysis). Data are presented as mean  $\pm$  S.E. 1 = Cloisite®, 2 = HNT, and 3 = MWCNT.

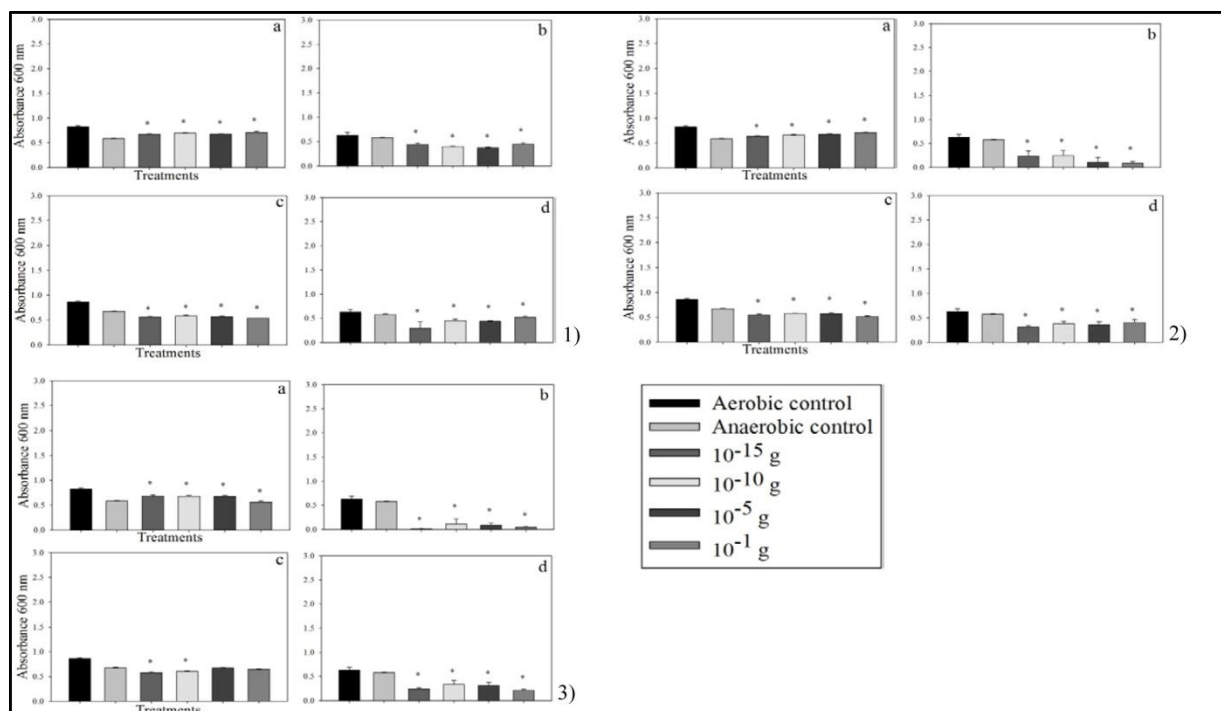


**Figure 21: LB toxicity (broth) test *S. typhimurium* SGSC 1336 *oxyR*.** Strains were evaluated under varying conditions: a) dark and aerobic, b) light and aerobic, c) dark and anaerobic, and d) light and anaerobic. The Kruskal-Wallis One Way Analysis of Variance on Ranks (non-parametric ANOVA) was performed to indicate significance among different groups. The \* indicates significance with the Holm-Sidak t- test ( $P < 0.05$ ) when treatments were compared to the appropriate control (aerobic treatments compared only to aerobic control and vice versa; the other control was used as a comparison only and was kept out of all statistical analysis). Data are presented as mean  $\pm$  S.E. 1 = Cloisite®, 2 = HNT, and 3 = MWCNT.

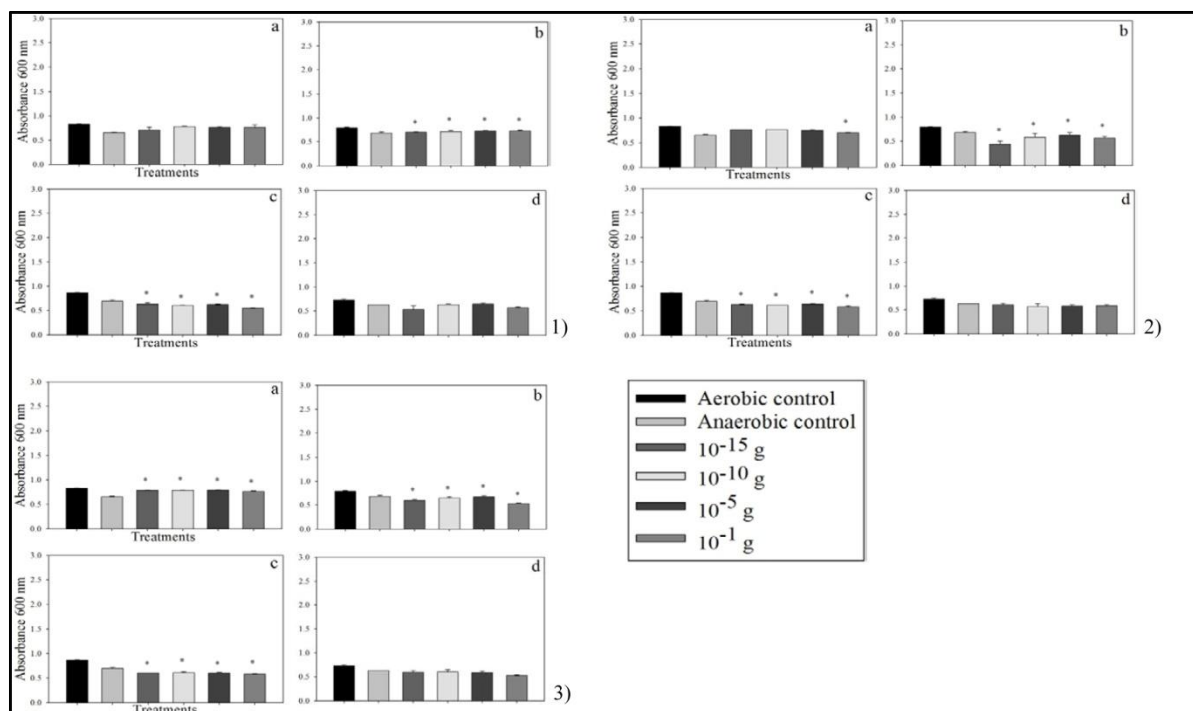


**Figure 22: LB toxicity (broth) test *S. typhimurium* SGSC 2618 *rpoS*.** Strains were evaluated under varying conditions: a) dark and aerobic, b) light and aerobic, c) dark and anaerobic, and d) light and anaerobic. The Kruskal-Wallis One Way Analysis of Variance on Ranks (non-parametric ANOVA) was performed to indicate significance among different groups. The \* indicates significance with the Holm-Sidak t- test ( $P < 0.05$ ) when treatments were compared to the appropriate control (aerobic treatments compared only to aerobic control and vice versa; the other control was used as a comparison only and was kept out of all statistical analysis). Data are presented as mean  $\pm$  S.E. 1 = Cloisite®, 2 = HNT, and 3 = MWCNT.

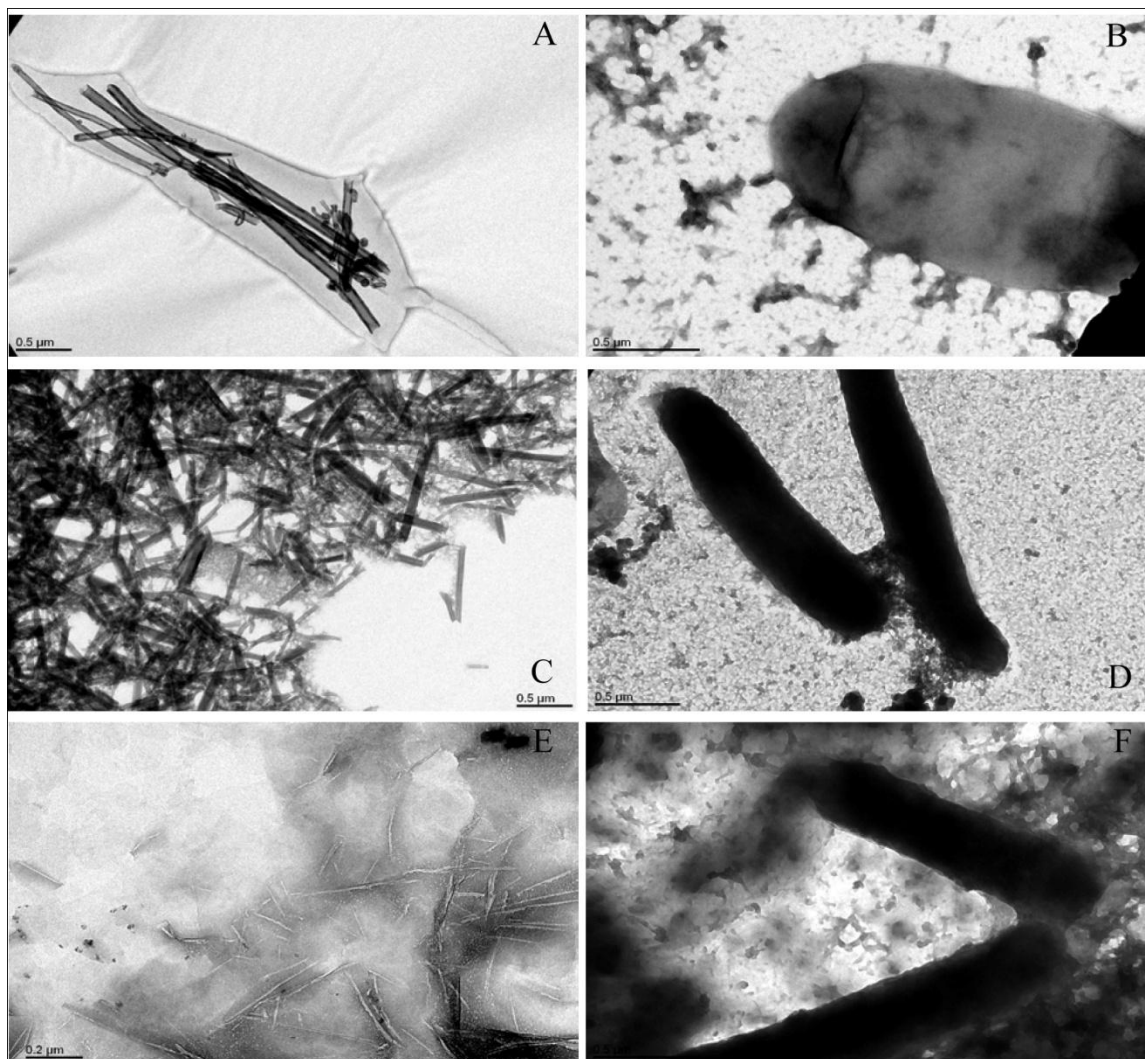


**Figure 23: Transmission electron images of the Cloisite®, HNT, and MWCNTs with and without *S. typhimurium* LT-2.** A) MWCNT magnified at 40k, B) MWCNT with *S. typhimurium* LT-2 magnified at 75k, C) HNT magnified at 40k, D) HNT with *S. typhimurium* LT-2 magnified at 60k, E) Cloisite® magnified at 100k, and F) Cloisite® with *S. typhimurium* LT-2 magnified at 75k. All images produced by Alissa Savage and the Texas State Biology Imaging Lab.

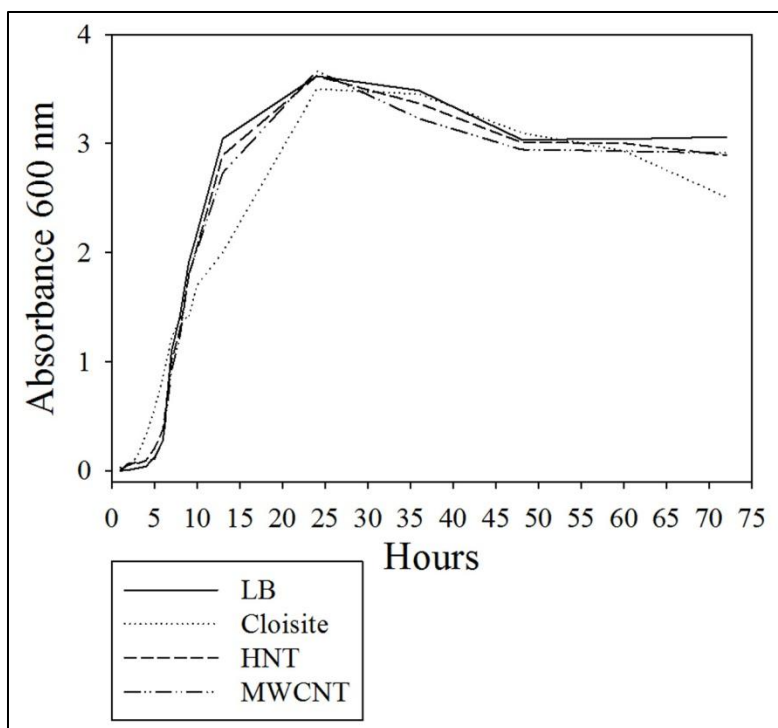


Figure 24: *E. coli* BW25113 growth curve.

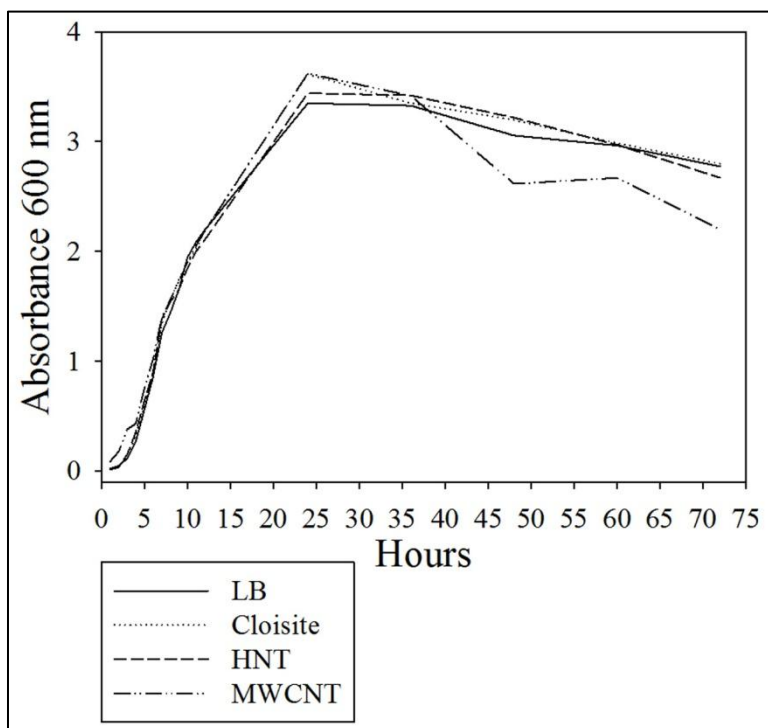


Figure 25: *E. coli* BW25113 *oxyR*- growth curve.

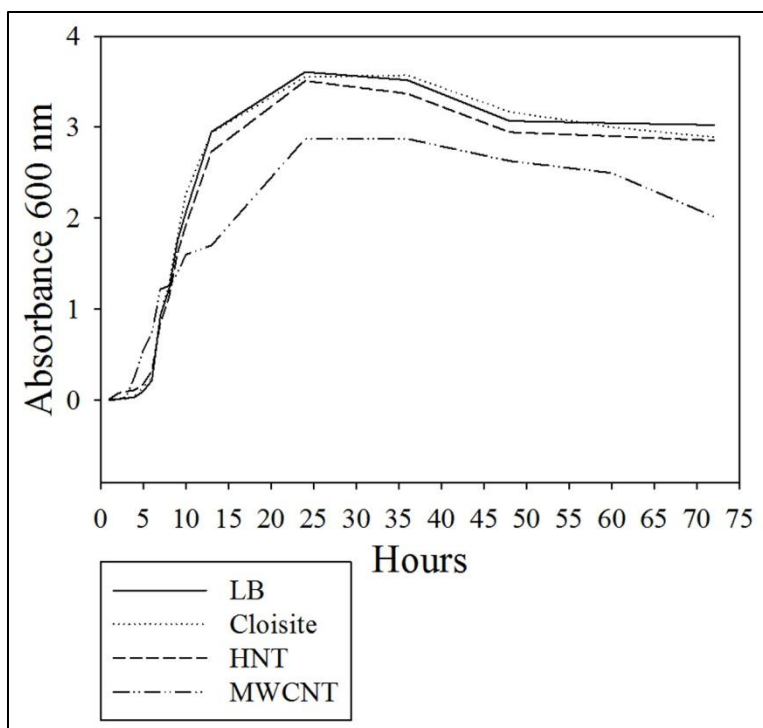


Figure 26: *E. coli oxyR/pCA24N* growth curve.

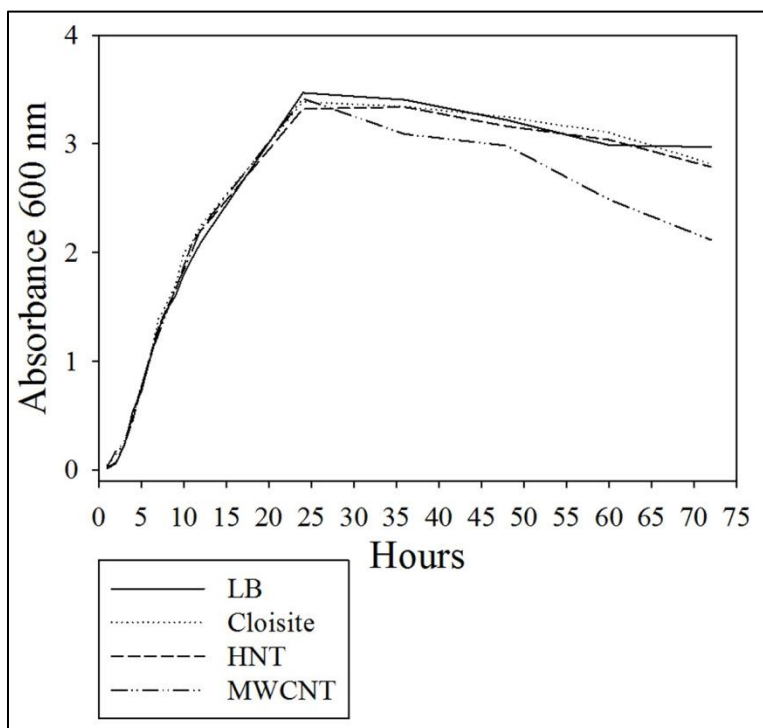


Figure 27: *E. coli* BW25113 *oxyR/pCA24N-oxyR* growth curve.

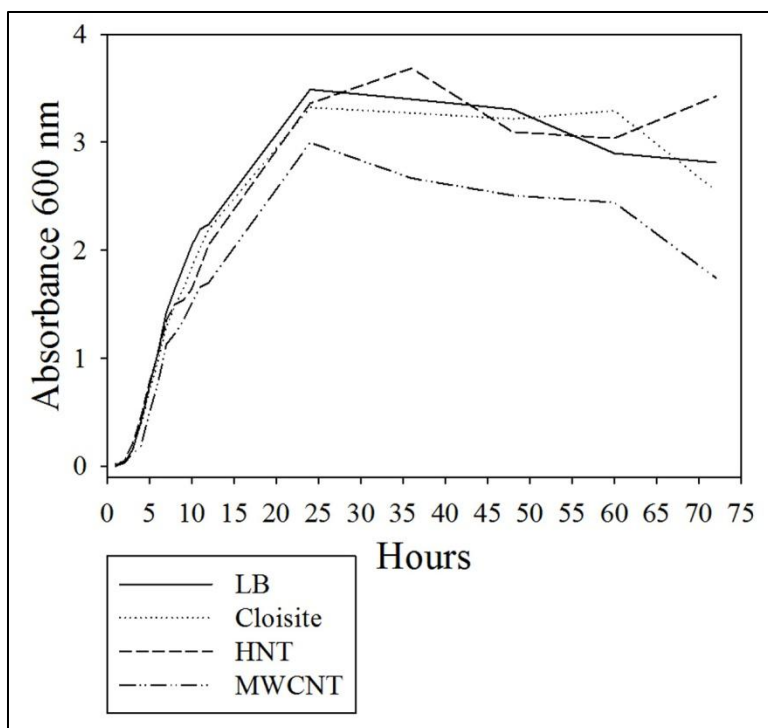


Figure 28: *E. coli* MG1655 growth curve.

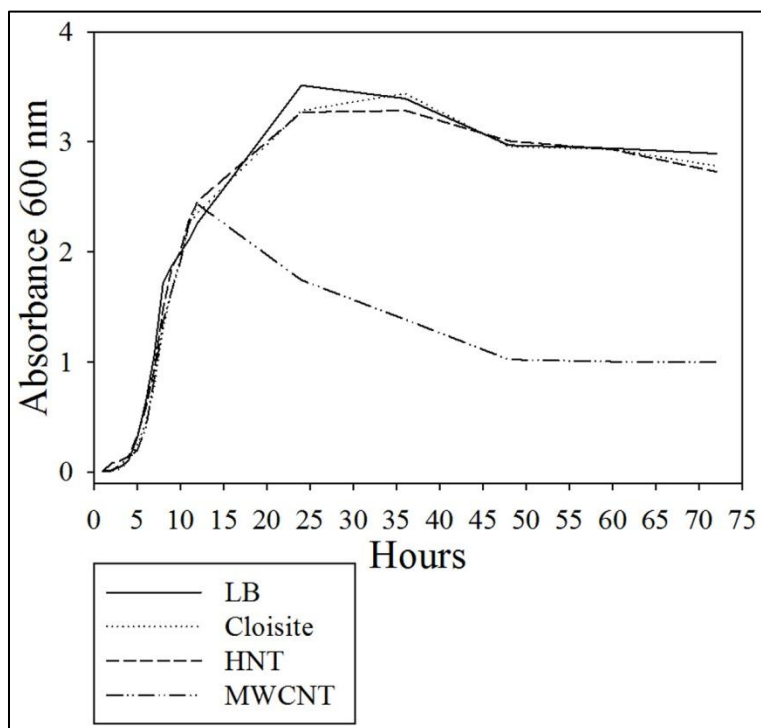


Figure 29: *E. coli* ZK1000 growth curve.

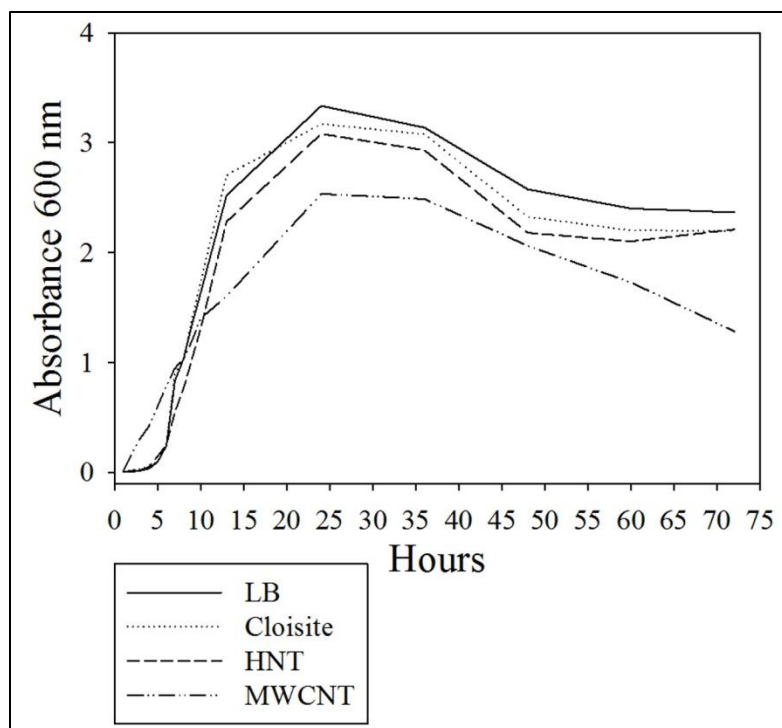


Figure 30: *S. typhimurium* TA102 growth curve.

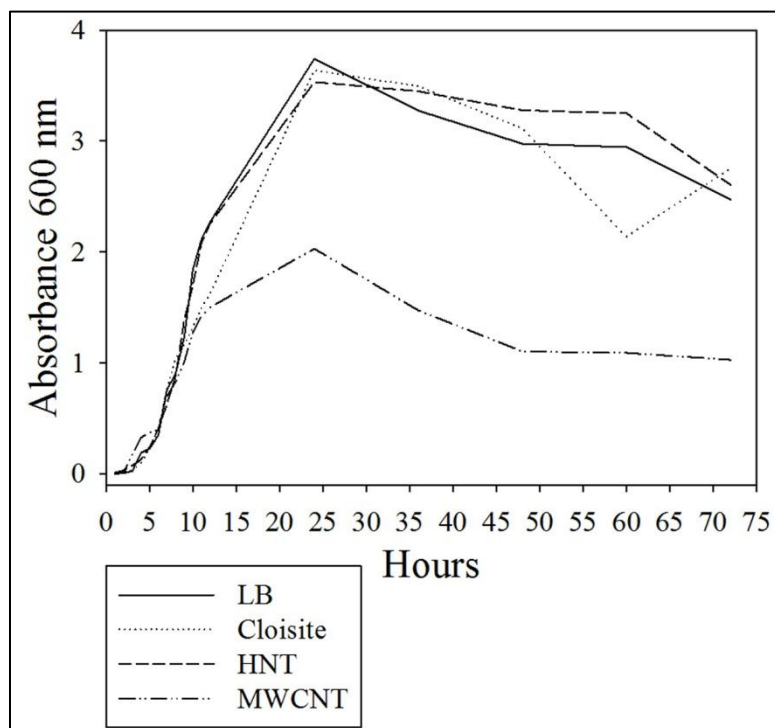


Figure 31: *S. typhimurium* TA1537 growth curve.

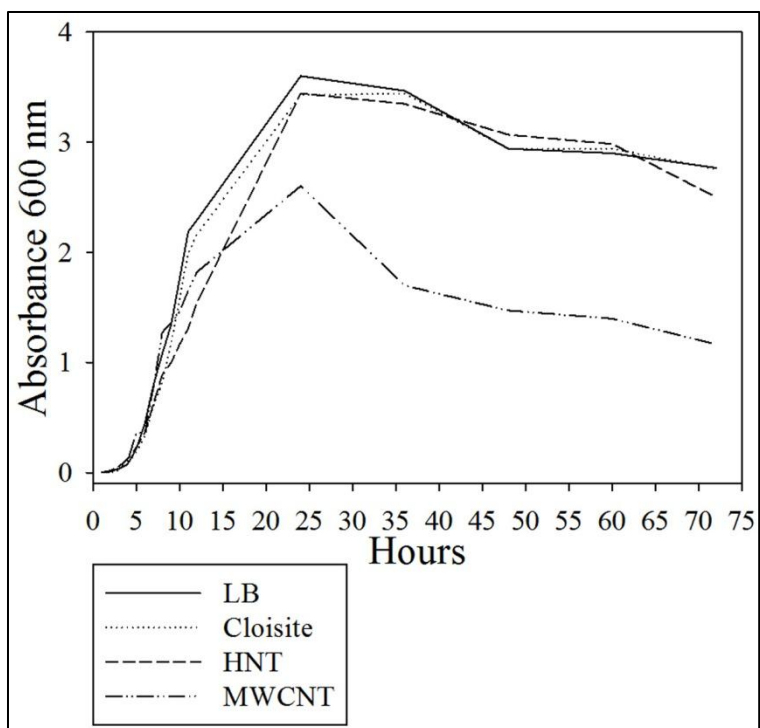


Figure 32: *S. typhimurium* TA1538 growth curve.

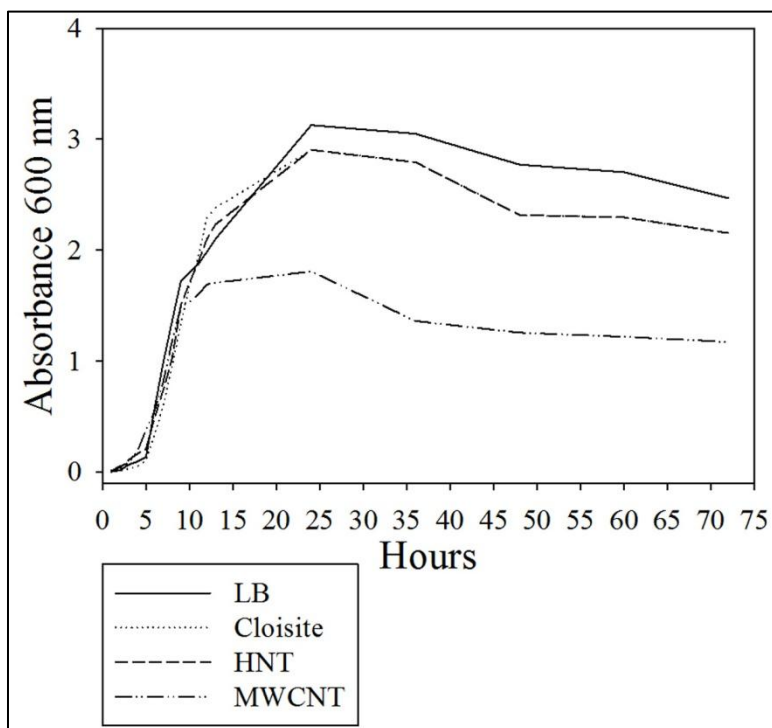


Figure 33: *S. typhimurium* LT-2 growth curve.

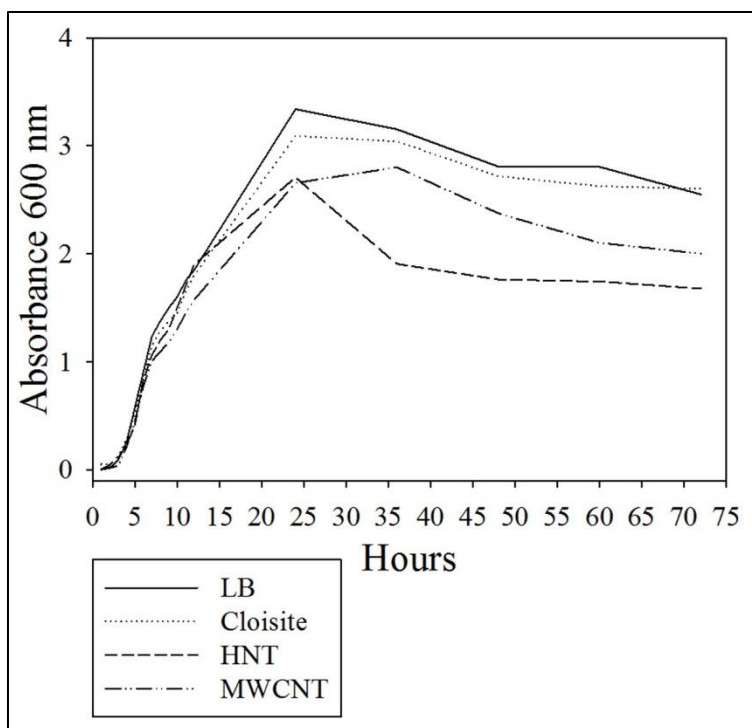


Figure 34: *S. typhimurium oxyR* growth curve.

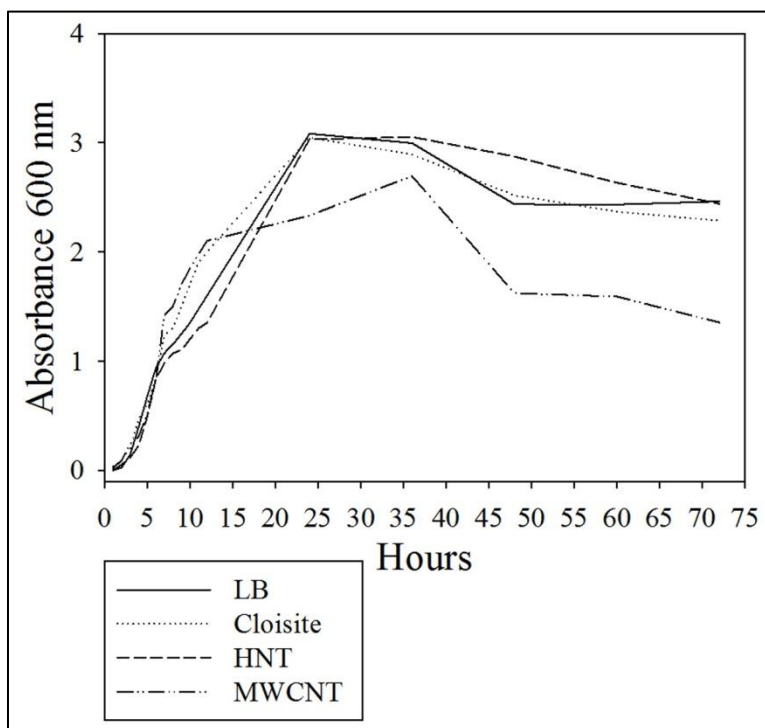


Figure 35: *S. typhimurium SGSC 2618 rpoS* growth curve.

## LITERATURE CITED

1. **Ames, B.N., F.D. Lee, and W.E. Durston.** 1973. An improved bacterial test system for the detection and classification of mutagens and carcinogens. *Proceedings of the National Academy of Sciences* **70(3)**: 782-786.
2. **Anonymous.** 2001. Halloysite. Mineral Data Publishing. Version 1.2.
3. **Anonymous.** 2001. Montmorillonite. Mineral Data Publishing.
4. **Anonymous.** Revised on May 8, 2009. Material Safety Data Sheet. NanoLab, Inc.
5. **Auffan, M., J. Rose, M.R. Wiesner, and J. Bottero.** 2009. Chemical stability of metal nanoparticles: A parameter controlling their potential cellular toxicity in vitro. *Environmental Pollution* **157(4)**: 1127-1133.
6. **Behra, R. and H. Krug.** 2008. Nanoparticles at large. *Nanoecotoxicology* **3**: 253-254.
7. **Bohannon, Dian, N. Connell, J. Keener, A. Tormo, M. Espinosa-Urgel, M. Mercedes Zambrano, and R. Kolter.** 1991. Stationary-phase-inducible 'gearbox' promoters: differential effects of *katF* mutations and role of  $\sigma^{70}$ . *Journal of Bacteriology* **173(14)**: 4482-4492.
8. **Bottini, M., S. Bruckner, K. Nika, N. Bottini, S. Bellucci, A. Magrini, A. Bergamaschi, and T. Mustelin.** 2006. Multi-walled carbon nanotubes induce T lymphocyte apoptosis. *Toxicology Letters* **160(2)**: 121-126.
9. [Cometicsinfo.org](http://Cometicsinfo.org)
10. **Dick, C.A., D.M. Brown, K. Donaldson, and V. Stone.** 2003. The role of free radicals in the toxic and inflammatory effects of four different ultrafine particle types. *Inhalation Toxicology* **15**: 39-52.
11. **EPA.** 2004. Air quality criteria for particulate matter (Vol. III) 600/P-95-001cF. Washington, DC 20460: Office of Research and Development.
12. **Federici G., B.J. Shaw, and R.D. Handy.** 2007. Toxicity of titanium dioxide nanoparticles to rainbow trout (*Oncorhynchus mykiss*): gill injury, oxidative stress, and other physiological effects. *Aquatic Toxicology* **84**: 415-30.

13. **Gurr, J.R., A.S.S. Wang, C.H. Chen, and K.Y. Jan.** 2005. Ultrafine titaniumdioxide particles in the absence of photoactivation can induce oxidative damage to human bronchial epithelial cells. *Toxicology* **213**: 66-73.
14. **Gwinn, M.R. and V. Vallyathan.** 2006. Nanoparticles: Health effects - pros and cons. *Environmental Health Perspectives* **114(12)**: 1818-1825.
15. **Hebrard, M., J.P.M. Viala, S. Meresse, F. Barras, and L. Aussel.** 2009. Redundant Hydrogen Peroxide Scavengers Contribute to *Salmonella* Virulence and Oxidative Stress Resistance. *Journal of Bacteriology* **191(14)**: 4605-4614.
16. **Hamilton Jr., R.F., S.A. Thakur, and A. Holian.** 2008. Silica binding and toxicity in alveolar macrophages. *Free Radical Biology and Medicine* **44**: 1246-1258.
17. **Herrera, P., R. Burghardt, H.J. Huebner, and T.D. Phillips.** 2004. The efficacy of sand-immobilized organoclays as filtration bed materials for bacteria. *Food Microbiology* **21**: 1-10.
18. **Holbrook, D.R., K.E. Murphy, J.B. Morrow, and Ken D. Cole.** 2008. Trophic Transfer of nanoparticles in a simplified invertebrate food web. *Nature Nanotechnology* **3**: 352-355.
19. **Hu, C. and M. Xia.** 2006. Adsorption and antibacterial effect of copper-exchanged montmorillonite on *Escherichia coli* K88. *Applied Clay Science* **31**: 1810-184.
20. **Hu, C.H., Z.R. Xu, and M.S. Xia.** 2005. Antibacterial effect of Cu<sup>2+</sup>-exchanged montmorillonite on *Aeromonas hydrophila* and discussion on its mechanism. *Veterinary Microbiology* **109**: 83-88.
21. **Jain, A.K., N.K. Mehra, N. Lodhi, V. Dubey, D.K. Mishra, P.K. Jain, and N.K. Jain.** 2007. Carbon nanotubes and their toxicity. *Nanotoxicology* **1(3)**: 167-197.
22. **Joussein, E., S. Petit, J. Churchman, B. Theng, D. Righi, and B. Delvaux.** 2005. Halloysite clay minerals – A review. *ClayMinerals* **40(4)**: 383-426.
23. **Kerr, Paul F.** 1952. Formation and occurrence of clay minerals. *Clays and Clay Minerals* **1**: 19-32.
24. **Keyhani, E., F. Abdi-Oskouei, F. Attar, and J. Keyhani.** 2006. DNA Strand Breaks by Metal-Induced Oxygen Radicals in Purified *Salmonella typhimurium* DNA. *Annals of the New York Academy of Sciences* **1091**: 52-64.
25. **Khanna, M. and G. Stotzky.** 1992. Transformation of *Bacillus subtilis* by DNA Bound on Montmorillonite and Effect of DNase on the Transforming Ability of Bound DNA. *Applied and Environmental Microbiology* **58(6)**: 1930-1939.

26. **Klaper R., J. Crago, J. Barr, D. Arndt, K. Setyowati, and J. Chen.** 2009. Toxicity biomarker expression in daphnids exposed to manufactured nanoparticles: changes in toxicity with functionalization. *Environmental Pollution* **157**: 1152-1156.
27. **Levin, D.E., M. Hollstein, M.F. Christman, E.A. Schwiers, and B.N. Ames.** 1982. A new *Salmonella* tester strain (TA102) with A-T base pairs at the site of mutation detects oxidative mutagens. *Proceedings of the National Academy of Sciences* **79**: 7445-7449.
28. **Lin, W., Y.W. Huang, X.D. Zhou, and Y. Ma.** 2006. In vitro toxicity of silica nanoparticles in human lung cancer cells. *Toxicology and Applied Pharmacology* **217**: 252-259.
29. **Loewen, P.C.** 1984. Isolation of catalase-deficient *Escherichia coli* mutants and genetic mapping of *katE*, a locus that affects catalase activity. *Journal of Bacteriology* **157**: 622-626.
30. **Long T.C., N. Saleh, R.D. Tilton, G.V. Lowry, and B. Veronesi.** 2006. Titanium dioxide (P25) produces reactive oxygen species in immortalized brain microglia (BV2): implication for nanoparticle neurotoxicity. *Environmental Science and Technology* **40**: 4346-52.
31. **Luo, P., Y. Zhao, B. Zhang, J. Liu, Y. Yang, and J. Liu.** 2010. Study on the adsorption of Neutral Red from aqueous solution onto halloysite nanotubes. *Water Research* **44**: 1489-1497.
32. **Maenosono, S., T. Suzuki, and S. Saita.** 2007. Mutagenicity of water soluble FePt nanoparticles in Ames test. *The Journal of Toxicological Sciences* **32(5)**: 575-579.
33. **Magana, S.M., P. Quintana, D.H. Aguilar, J.A. Toledo, C. Angeles-Chavez, M.A. Cortes, L. Leon, Y. Freile-Pelegrin, T. Lopez, and R.M. Torres Sanchez.** 2008. Antibacterial activity of montmorillonites modified with silver. *Journal of Molecular Catalysis A: Chemical* **281(1-2)**: 192-199.
34. **Malachová, K., P. Praus, Z. Pavlíčková, and M. Turicová.** 2009. Activity of antibacterial compounds immobilised on montmorillonite. *Applied Clay Science* **43**: 364-368.
35. **Mazzola, L.** 2003. Commercializing Nanotechnology. *Nature Biotechnology* **21(10)**: 1137-1143.
36. **McCann, J., N.E. Spingarn, J. Kabori, and B.N. Ames.** 1975. Detection of carcinogens as mutagens: Bacterial Tester Strains with R factor plasmids. *Proceedings of the National Academy of Sciences* **72(3)**: 979-983.

37. **McCann, J., E. Choi, E. Yamasaki, and B.N. Ames.** 1975. Detection of carcinogens as mutagens in the *Salmonella*/microsome test: Assay of 300 Chemicals. *Proceedings of the National Academy of Sciences* **72(12)**: 5135-5139.
38. **Meng, N., N. Zhou, S. Zhang, and J. Shen.** 2009. Synthesis and antifungal activities of polymer/ montmorillonite–terbinafine hydrochloride nanocomposite films, *Applied Clay Science* **46(2)**: 136-140.
39. **NanoLab, Inc.** 55 Chapel St. Newton, MA 02458 USA Phone (617) 581-6747 Fax (617) 581-6749 [www.nano-lab.com](http://www.nano-lab.com)
40. **NaturalNano, Inc.** 832 Emerson St. Rochester, NY 14613 Telephone: 585.267.4848.
41. **Nel, A., T. Xia, L. Mädler, and N. Li.** 2006. Toxic potential of materials at the nanolevel. *Science* **311**: 622-627.
42. **Nzengung, V.A., E.A. Voudrias, P. Nkedi-Kizza, J.M. Wampler, and C.E. Weaver.** 1996. Organic cosolvent effects on sorption equilibrium of hydrophobic organic chemicals by organoclays. *Environmental Science and Technology* **30**: 89-96.
43. **Oberdörster, Eva.** 2004. Manufactured Nanomaterials (Fullerenes, C60) Induce Oxidative Stress in the Brain of Juvenile Largemouth Bass. *Environmental Health Perspectives* **112(10)**: 1058-1062.
44. **Oberdörster, Günter, V. Stone, and K. Donaldson.** 2007. Toxicology of nanoparticles: A historical perspective. *Nanotoxicology* **1(1)**: 2-25.
45. **Powers, K.W., M. Palazuelos, B.M. Moudgil, and S.M. Roberts.** 2007. Characterization of the size, shape, and state of dispersion of nanoparticles for toxicological studies. *Nanotoxicology* **1(1)**: 42-51.
46. **Qu, S., F. Huang, S.N. Yu, G. Chen, and J.L. Kong.** 2008. Magnetic removal of dyes from aqueous solution using multi-walled carbon nanotubes filled with Fe<sub>2</sub>O<sub>3</sub> particles. *Journal of Hazardous Materials* **160(2-3)**: 643-647.
47. **Reilly, R.M.** 2007. Carbon Nanotubes: Potential benefits and risks of nanotechnology in nuclear medicine. *Journal of Nuclear Medicine* **48(7)**: 1039-1042.
48. **Ryan, J.J., H.R. Bateman, A. Stover, G. Gomez, S.K. Norton, W. Zhao, L.B. Schwartz, R. Lenk, and C.L. Kepley.** 2007. Fullerene Nanomaterials Inhibit the Allergic Response. *Journal of Immunology* **179**: 665-672.

49. **Sawai, J., H. Kojima, F. Kano, H. Igarashi, A. Hashimoto, E. Kawada, T. Kokugan, and M. Shimizu.** 1998. Short communication: Ames assay with *Salmonella typhimurium* TA102 for mutagenicity and antimutagenicity of metallic oxide powders having antibacterial activities. *World Journal of Microbiology and Biotechnology* **14**: 773-775.
50. **Seaver, L.C. and J.A. Imlay.** 2001. Alkyl hydroperoxide reductase is the primary scavenger of endogenous hydrogen peroxide in *Escherichia coli*. *Journal of Bacteriology* **183**: 7173-7181.
51. **Southern Clay Products, Inc.** 1212 Church Street Gonzales, Texas 78629 Tel: 1.800.324.2891 Direct Line: 1.830.672.2891 Fax: 1.830.672.1920.
52. **Storz, G. and R. Hengge-Aronis (ed.).** 2000. Bacterial stress responses. American Society of Microbiology Press, Washington, D.C.
53. **Stotzky, G.** 1989. Gene transfer among bacteria in soil. p. 165–222. *In* S.B. Levy and R.V. Miller (ed.) Gene transfer in the environment. McGraw-Hill, New York.
54. **Swaby, R. J.** 1949. The relationship between micro-organisms and soil aggregation. *The Journal of General Microbiology* **3**: 236-254.
55. **Systat Software, Inc.** 1735 Technology Drive, Ste. 430 San Jose, CA 95110.
56. **Truesdail, S.E., J. Lukasik, S.R. Farrah, D.O. Shah, and R.B. Dickson.** 1998. Analysis of bacterial deposition on metal (hydr)oxide-coated sand filter media. *Journal of Colloid and Interface Science* **203**: 369-378.
57. **USGS.** Smectite Group. A laboratory manual for x-ray powder diffraction. U.S. Geological Survey Open-file report 01-041. Last modified October 2001.
58. **Wang, X., Q. Li, J. Xie, Z. Jin, J. Wang, Y. Li, K. Jiang, and S. Fan.** 2009. Fabrication of ultralong and electrically uniform single-walled carbon nanotubes on clean substrates. *Nano Letters* **9(9)**: 3137-3141.
59. **Yoo, A., S.W. Kim, J.E. Yu, Y.H. Kim, J. Cha, J. Oh, S.K. Eo, J.H. Lee, and H.Y. Kang.** 2007. Requirement of Fur for the Full Induction of dps Expression in *Salmonella enterica* Serovar Typhimurium. *Journal of Microbiology and Biotechnology* **17(9)**: 1452-1459.
60. **Yu, M., O. Lourie, M.J. Dyer, K. Moloni, T.F. Kelly, and R.S. Ruoff.** 2000. Strength and breaking mechanism of multiwalled carbon nanotubes under tensile load. *Science* **287**: 637-640.

61. **Yuzuki, N.S. Wakuri, K. Sakamoto, and N. Tanaka.** 1997. The photogenotoxicity of titanium dioxide particles. *Mutation Research/Genetic Toxicology and Environmental Mutagenesis* **394(1-3)**: 125-132.

## VITA

Alicia Ann Taylor was born in Grand Prairie, Texas on September 9, 1985 to Diane and Jeffrey Taylor. Following graduation from Martin High School in Arlington, Texas in 2004, she attended the University of North Texas in Denton, Texas where she majored in Biology. Alicia completed her Bachelor of Science degree in December 2007. After graduation, she worked at Bio-Aquatic Testing, Inc. as an aquatic toxicology laboratory technician. In August 2008, Alicia attended Texas Woman's University in Denton, Texas as a non-degree seeking graduate student where she completed a semester of graduate coursework and was a graduate assistant for Microbiology for Nursing Majors. In January 2009, she moved to San Marcos, Texas to pursue her M.S. in Biology at Texas State University-San Marcos. As a graduate student, she worked as an instructional assistant for Microbiology and Microbial Physiology and Genetics. Additionally, she served as the Microbiology Laboratory Coordinator for Dr. Robert McLean in the Department of Biology, Texas State University-San Marcos. Alicia received the George H. Meyer Award in Microbiology in 2010.

Permanent Address: 4111 Green Acres Circle

Arlington, Texas 76017

[aliciaataylor@gmail.com](mailto:aliciaataylor@gmail.com)

This thesis was typed by Alicia A. Taylor